

This discussion paper is/has been under review for the journal Geoscientific Model Development (GMD). Please refer to the corresponding final paper in GMD if available.

GMDD

4, 2791–2847, 2011

Description of EQSAM4: gas-liquid-solid partitioning model for global simulations

S. Metzger¹, B. Steil¹, L. Xu², J. E. Penner², and J. Lelieveld^{1,3,4}

¹Max Planck Institute for Chemistry, Mainz, Germany

²University of Michigan, Ann Arbor, Michigan, USA

³The Cyprus Institute, Nicosia, Cyprus

⁴King Saud University, Riyadh, Saudi Arabia

Received: 28 September 2011 – Accepted: 20 October 2011 – Published: 24 October 2011

Correspondence to: S. Metzger (swen.metzger@mpic.de)

Published by Copernicus Publications on behalf of the European Geosciences Union.

Discussion Paper | Discussion Paper

EQSAM4 model
description

S. Metzger et al.

Title Page

Abstract

Introduction

Conclusions

References

Tables

Figures

◀

▶

◀

▶

Back

Close

Full Screen / Esc

Printer-friendly Version

Interactive Discussion



Abstract

We introduce version 4 of the EQuilibrium Simplified Aerosol Model (EQSAM4), which is part of our aerosol chemistry-microphysics module (GMXe) and chemistry-climate model (EMAC). We focus on the relative humidity of deliquescence (RHD) based water uptake of atmospheric aerosols, as this is important for atmospheric chemistry and climate modeling, e.g. to calculate the aerosol optical depth (AOD). Since the main EQSAM4 applications will involve large-scale, long-term and high-resolution atmospheric chemistry-climate modeling with EMAC, computational efficiency is an important requirement. EQSAM4 parameterizes the composition and water uptake of multicomponent atmospheric aerosols by considering the gas-liquid-solid partitioning of single and mixed solutes. EQSAM4 builds on analytical, and hence CPU efficient, aerosol hygroscopic growth parameterizations to compute the aerosol liquid water content (AWC). The parameterizations are described in the companion paper (Metzger et al., 2011) and only require a compound specific coefficient v_i to derive the single solute molality and the AWC for the whole range of water activity (a_w). v_i is pre-calculated and applied during runtime by using internal look-up tables. Here, the EQSAM4 equilibrium model is described and compared to the more explicit thermodynamic model ISORROPIA II. Both models are imbedded in EMAC/GMXe. Box model inter-comparisons, including the reference model E-AIM, and global simulations with EMAC show that gas-particle partitioning, including semi-volatiles and water, is in good agreement. A more comprehensive box model inter-comparison of EQSAM4 with EQUISOLV II is subject of the revised publication of Xu et al. (2009), i.e. Xu et al. (2011).

1 Introduction

The most comprehensive description of hygroscopic particle growth of atmospheric aerosols is provided by models that calculate the full gas-liquid-solid partitioning, i.e. the composition and state of the aerosol over the wide ranges of temperature and

EQSAM4 model description

S. Metzger et al.

[Title Page](#)

[Abstract](#)

[Introduction](#)

[Conclusions](#)

[References](#)

[Tables](#)

[Figures](#)

[◀](#)

[▶](#)

[◀](#)

[▶](#)

[Back](#)

[Close](#)

[Full Screen / Esc](#)

[Printer-friendly Version](#)

[Interactive Discussion](#)



EQSAM4 model description

S. Metzger et al.

[Title Page](#)[Abstract](#)[Introduction](#)[Conclusions](#)[References](#)[Tables](#)[Figures](#)[◀](#)[▶](#)[◀](#)[▶](#)[Back](#)[Close](#)[Full Screen / Esc](#)[Printer-friendly Version](#)[Interactive Discussion](#)

2006; Feng and Penner, 2007), or a General-Circulation Model, GCM (e.g. Adams et al., 2001; Jacobson, 2001; Liao et al., 2003; Martin et al., 2004; Rodriguez and Dab-dub, 2004; Lauer et al., 2005; Liao and Seinfeld, 2005; Liao et al., 2006; Bauer et al., 2007a, b; Luo et al., 2007; Metzger et al., 2007; Pringle et al., 2010; Brühl et al., 2011; Pozzer et al., 2011). However, despite the model development history of EQMs, computational efficiency combined with accuracy and flexibility regarding the number of chemical compounds that can be considered remains to be a key development in global atmospheric aerosol-chemistry-climate modeling.

Here we introduce version 4 of the Equilibrium Simplified Aerosol Model (EQSAM4), which is part of an aerosol chemistry-microphysics module (GMXe) and a chemistry-climate model (EMAC). Section 2.1 describes the EQSAM4 parameterization of the composition and water uptake of multicomponent atmospheric aerosols, by considering the gas-liquid-solid partitioning of single and mixed solutes. The analytical, and hence CPU efficient, single solute parameterizations are summarized in Sect. 2.2, described in greater detail in the companion paper (Metzger et al., 2011, abbreviated in the following as M2011). The corresponding mixed solution parameterizations and the computational algorithm are summarized in Sects. 2.3. and 2.4, respectively. Section 3.1 presents box model applications of EQSAM4 and the more explicit thermodynamic model ISORROPIA II, which are compared against the results of the thermodynamic reference model E-AIM for major single salt solutions (i.e. containing NaCl, NH₄NO₃, NH₄Cl, (NH₄)₂SO₄, NH₄HSO₄, Na₂SO₄, NaNO₃), and the corresponding mixed solutions. Section 3.2 complements the box model results with results of a global modeling application of EQSAM4 and ISORROPIA II, with both models imbedded in EMAC/GMXe. We conclude with Sect. 4. For a more comprehensive box model inter-comparison of EQSAM4 and other EQMs we refer to the revised publication of Xu et al. (2009), i.e. Xu et al. (2011).

EQSAM4 model description

S. Metzger et al.

[Title Page](#)

[Abstract](#)

[Introduction](#)

[Conclusions](#)

[References](#)

[Tables](#)

[Figures](#)

◀

▶

◀

▶

[Back](#)

[Close](#)

[Full Screen / Esc](#)

[Printer-friendly Version](#)

[Interactive Discussion](#)



2 Model description

Version 4 of the EQuilibrium Simplified Aerosol Model (EQSAM4) is a solubility based gas-liquid-solid equilibrium partitioning model and a major revision of EQSAM3 with many improvements, although the overall analytical structure of EQSAM3 (Metzger et al., 2007) is largely unchanged. In contrast to other thermodynamic gas/aerosol equilibrium models, only a minimum number of iterations are required to solve the equilibrium reactions and the gas-liquid-solid partitioning of single solute or mixed solutions. Moreover, all relevant solution properties such as the solute molality (μ_s), activity coefficients of (semi-)volatile compounds (γ_s), relative humidity of deliquescence (RHD), relative humidity of crystallization or efflorescence (RHE) and the associated aerosol water of binary and multi-component aerosol mixtures are parameterized using analytical functions, which depend at a specific relative humidity (RH) and temperature (T) only on a single solute specific coefficient v_i . v_i is pre-calculated at the model start from the chemical compound's T -dependent RHD and saturation solubility μ_s^{sat} , and applied during runtime by using compound and T -dependent internal look-up tables of v_i .

A key-feature of the EQSAM4 parameterizations is that the solute molality does not depend on the water content of the solution. Therefore, all solution properties can be calculated at a given RH and T only once for each compound, independent of whether single or mixed solutions are involved. During model set up all compounds can be individually switched on or off, and during run-time only the selected compounds are considered in internal compound loops. Calculations are skipped if a compound cannot form, e.g. because the required cation or anion has zero concentration. Both options can significantly enhance speed in global modeling applications, while the open architecture allows the user to easily incorporate new compounds or modify existing ones.

The compounds currently implemented are listed in Table 1. EQSAM4 is positive-definite, mass- and charge-conserving, and considers the so-called hysteresis loop for aerosols that transfer between dry and moist environments.

EQSAM4 model description

S. Metzger et al.

[Title Page](#)

[Abstract](#)

[Introduction](#)

[Conclusions](#)

[References](#)

[Tables](#)

[Figures](#)

◀

▶

◀

▶

[Back](#)

[Close](#)

[Full Screen / Esc](#)

[Printer-friendly Version](#)

[Interactive Discussion](#)



EQSAM4 model description

S. Metzger et al.

[Title Page](#)[Abstract](#)[Introduction](#)[Conclusions](#)[References](#)[Tables](#)[Figures](#)[◀](#)[▶](#)[◀](#)[▶](#)[Back](#)[Close](#)[Full Screen / Esc](#)[Printer-friendly Version](#)[Interactive Discussion](#)

For the hysteresis loop we assume that atmospheric aerosols (i) instantaneously take up water when solids deliquesce, i.e. in case the RH increases above the RHD of individual solid compounds (following the lower bound of the hysteresis loop), while (ii) aerosol water evaporates until crystallization occurs at the RHE point (following the upper bound of the hysteresis loop); at lower RH the aerosol water decreases instantaneously to zero. At the RHD, the solution is saturated and supersaturated at lower RH. An electrolyte is assumed solid when the RH is below its RHD (deliquescence branch) or RHE (efflorescence branch) when the solid precipitates from solution, whereas a solid is not allowed to form when the RH increases above the RHD or RHE, respectively. In both cases (efflorescence or deliquescence), the solute concentration increases with decreasing RH and decreasing aerosol water, while the total aerosol liquid water content usually increases with increasing RH and constant solute concentration, or constant RH and increasing solute concentration (mass or number). The aerosol particle is assumed dry when the RH is below the lowest RHD (deliquescence branch) or RHE (efflorescence branch) of all solutes present in the mixed solution; and in transport modeling applications, if additionally the total aerosol water from the previous model time-step is zero.

2.1 Method of parameterizing the gas-liquid-solid partitioning

The single and mixed solution concentrations are calculated by considering a neutralization reaction order, assuming chemical and thermodynamical equilibrium. The neutralization reaction order is automatically pre-determined during model start up for the selected species, which are considered in the gas-liquid-solid equilibrium partitioning calculations. The neutralization reaction order is based on the so-called salting-out effect of salt solutes and accounts for the order and degree to which ions bind water (Hofmeister, 1988). Two options are available:

1. Prescribed according to an adopted (T -independent) Hofmeister series;
2. Automatically determined based on the solute's T -dependent RHD or RHE values.

**EQSAM4 model
description**

S. Metzger et al.

[Title Page](#)[Abstract](#)[Introduction](#)[Conclusions](#)[References](#)[Tables](#)[Figures](#)[◀](#)[▶](#)[◀](#)[▶](#)[Back](#)[Close](#)[Full Screen / Esc](#)[Printer-friendly Version](#)[Interactive Discussion](#)

For (2) the neutralization order is automatically determined for a given temperature using the T -dependent RHD values of the selected electrolytes. The electrolyte with the lowest solubility (highest RHD) is assumed to be neutralized first. For both options the compounds with highest RHD precipitates from the solution first so that the solute ions (of the precipitating compound) are not available for further reactions. For the RHE order, the procedure is basically the same, only the ranking of salt solutes varies. On the other hand, if the reaction order is prescribed as in (1), the following constant (T -independent) ranking is assumed, in which the ions to the left are neutralized preferentially, i.e.:

- 10 – Anions: $\text{PO}_4^{3-} > \text{SO}_4^{2-} > \text{HSO}_4^- > \text{NO}_3^- > \text{Cl}^- > \text{Br}^- > \text{I}^- > \text{CO}_3^{2-} >$
 $\text{HCO}_3^- > \text{OH}^- > \text{CHO}_2^- > \text{C}_2\text{H}_3\text{O}_2^- > \text{C}_2\text{O}_4^{2-} > \text{C}_6\text{H}_5\text{O}_7^{3-}$
- Cations: $\text{Fe}^{3+} > \text{Mg}^{2+} > \text{Ca}^{2+} > \text{Na}^+ > \text{K}^+ > \text{NH}_4^+ > \text{H}^+$

This ranking is based on Hofmeister (1988) and our modeling experience. It assumes that the neutralization of compounds approximately follows their ability to precipitate from a mixture of solutes. This increases the effective concentration of the remaining ions so that they precipitate if saturation is reached, e.g. in case of decreasing RH and water activity. The advantage of the prescribed neutralization order is that the ranking can be varied very easily (e.g. to study the effect on the overall gas-aerosol partitioning), but there is no T -dependency, while the RHD (or RHE) order automatically involves a T -dependency, which is applied during runtime for the compounds for which data is available (see Sect. 2.2 for details). An inter-comparison between these two neutralization orders is presented in the revised publication of Xu et al. (2009, 2011). For both options, all salt solutes (cation-anion pairs) considered are ranked with respect to the preferred cation-anion neutralization and this index information is stored in an internal array, which is subsequently used as a look-up table during runtime, e.g. to obtain the corresponding ion and ion charge indices of the forming compounds (assuming charge balance). Then, during runtime, this index information is used for a given set

EQSAM4 model description

S. Metzger et al.

[Title Page](#)[Abstract](#)[Introduction](#)[Conclusions](#)[References](#)[Tables](#)[Figures](#)[◀](#)[▶](#)[◀](#)[▶](#)[Back](#)[Close](#)[Full Screen / Esc](#)[Printer-friendly Version](#)[Interactive Discussion](#)

2.2 Single solute parameterizations

The EQSAM4 parameterizations are a function of the solute specific coefficient v_i and RH.

2.2.1 The RH of deliquescence (RHD) and efflorescence (RHE) as a function of v_i

It is assumed that atmospheric aerosols absorb water vapor if the RH rises above the dimensionless relative humidity of deliquescence (RHD), or desorb water vapor until the RH decreases below the dimensionless relative humidity of efflorescence (RHE). The RHD refers to an equilibrium RH at which a dry and crystalline salt compound completely deliquesces due to water vapor uptake at sufficiently high RH. At the lower end the RHE refers to an equilibrium RH at which an aqueous (and potentially dissociated) salt compound completely dries again, i.e. it crystallizes due to evaporative loss of water at sufficiently low RH. Assuming equilibrium and solution saturation, it is implicit that phase partitioning takes place at RHD from entirely dry (and crystalline) to entirely wet (dissolved), and analogously for the RHE case. Thus, modeling the RHD and RHE can only approximate reality, since a non-equilibrium approach is not accounted for. Thus, any interim transition phase of single solutes is not considered, although they are to some degree captured by the modeling of mixed solutions (described in Sect. 2.3).

The RHD parameterization relates the solute solubility, i.e. the saturation molality of the dissolved solute, to RH by the solute specific coefficient v_i . According to Eq. (16b) of M2011, i.e. the (simplified) relation without the Kelvin-term is given by:

$$\text{RHD} = \left(1 + \mu_s^o \cdot M_w \cdot v_i \cdot \left[\frac{1}{\mu_s^o} \cdot \frac{1}{M_s \cdot (1/w_s - 1)} + B_{98} \right]^{v_i} \right)^{-1} \quad (1)$$

EQSAM4 model description

S. Metzger et al.

[Title Page](#)

[Abstract](#)

[Introduction](#)

[Conclusions](#)

[References](#)

[Tables](#)

[Figures](#)

[◀](#)

[▶](#)

[◀](#)

[▶](#)

[Back](#)

[Close](#)

[Full Screen / Esc](#)

[Printer-friendly Version](#)

[Interactive Discussion](#)



The RHE is parameterized accordingly, following Metzger and Lelieveld (2007) as:

$$\text{RHE} = 1 - \left(1 + \mu_s^o \cdot M_w \cdot v_i \cdot \left[\frac{1}{\mu_s^o} \cdot \frac{(1/w_s - 1)}{M_s} + B_{98} \right]^{v_i} \right)^{-1} \quad (2)$$

M_w and M_s denote the molar mass [kg/mol] of water and solute, and w_s [-] the mass fraction solubility. $\mu_s^o = 1$ [mol(solute)/kg(H₂O)] and the term B_{98} is:

$$B_{98} = 10^{\left[\frac{2}{v_i} - 2 \right]} = x \cdot w_s \quad (3)$$

with x an arbitrary variable used to relate B_{98} and w_s ; x follows if v_i is known. v_i is determined in Sect. 2.2.2. B_{98} refers to applications at RH ≤ 98 [%]. Note that the model default is using B_{98} rather than the complete A and B terms (defined in M2011 for which also the Kelvin-term is considered), since the B_{98} term allows us to solve the equations analytically, i.e. without iterations. The model has an option to consider the Kelvin-term, which uses the complete A and B terms and pre-calculated values of the solute molality (through look-up tables). This additional option is currently only validated for NaCl and (NH₄)₂SO₄ due to the lack of available data. This will be further investigated. Also note that the B_{98} term yields similar results as the Kelvin-term option for the important RH range RHD < RH ≤ 98 [%] (M2011).

To consider temperature dependency of the RHD and RHE values EQSAM4 applies the widely used T -dependency for major salt compounds (e.g. Wexler and Potukuchi, 1998):

$$\text{RHD}(T) = \text{RHD}(T_o) \cdot \exp \left[T_{\text{coef}} \cdot \left(\frac{1}{T} - \frac{1}{T_o} \right) \right] \quad (4)$$

For all compounds for which T -dependent RHD and w_s data are not available, no T -dependency is considered per default. However, EQSAM4 has an option

[Title Page](#)[Abstract](#)[Introduction](#)[Conclusions](#)[References](#)[Tables](#)[Figures](#)[◀](#)[▶](#)[◀](#)[▶](#)[Back](#)[Close](#)[Full Screen / Esc](#)[Printer-friendly Version](#)[Interactive Discussion](#)

to approximate a T -dependency for the solute solubility w_s following Metzger and Lelieveld (2007), i.e.

$$w_s(T) = w_s(T_o) \cdot \frac{T}{T_o} \quad (5)$$

- so that a T -dependency of the RHD can be calculated from Eqs. (5), (3) and (1), and for the RHE from Eqs. (5), (3) and (2). Only the default option explicitly accounts for different heat capacities of salt compounds by the use of T -coefficients. The T -coefficients and RHD values at $T_o = 298$ [K] are shown in Table 2 for compounds of which coefficients are available; values are the same as those used in ISORROPIA II (see Table 4 of Fountoukis and Nenes, 2007). RHD values at T_o and T -coefficients are unfortunately only available for the major inorganic salt compounds listed in Tables 1 and 2. Data for organic salt compounds are lacking, and T -coefficients for the RHE are not available for both inorganic or organic salt compounds. We therefore have included the option to estimate a T -dependency of both RHD and RHE from a parameterized T -dependency of the solute solubility using Eq. (5). However, this option is considered only for test purposes (e.g. sensitivity studies) as it requires evaluation and further development. Also, all non-bold RHD and all RHE values shown in Tables 3 and 4 are optional and indicative though similar to Metzger and Lelieveld (2007), since measurements are required for validation, in particular for the RHE values. For instance, a shape factor is currently not applied, though required for certain compounds to crystallize at the observed RHE. For example, the predicted RHE value of NaCl is higher than its RHD value, which can be corrected if a shape factor is applied. Thus, further improvement is foreseen. The RHE values corresponding to the compounds listed in Table 2 are partially evaluated in the revised publication of Xu et al. (2009, 2011). Missing compounds (Tables 3 and 4 compared to Table 1) are not considered for the liquid-solid-partitioning calculations, although they are included in the overall gas-aerosol partitioning (if selected), to account for their dry mass, which affects the overall hygroscopic growth factor and the derived aerosol size distribution and life-time.

EQSAM4 model description

S. Metzger et al.

[Title Page](#)[Abstract](#)[Introduction](#)[Conclusions](#)[References](#)[Tables](#)[Figures](#)[◀](#)[▶](#)[◀](#)[▶](#)[Back](#)[Close](#)[Full Screen / Esc](#)[Printer-friendly Version](#)[Interactive Discussion](#)

2.2.2 Determination of v_i

The dimensionless solute specific coefficient v_i [–] is obtained from the measured reference RHD (as used in Eq. 4) with the bisection method (described in Sect. 3 of M2011) for compounds for which a reference value is available, i.e. all compounds listed in Table 2. The same RHD values are indicated in bold in Table 3 (all values were re-calculated with Eq. 1 and are, in this case, identical to those of Table 2). For all compounds for which reference RHD values are not available, v_i is obtained from the solute's mass fraction solubility, w_s , following Metzger and Lelieveld (2007), by using Eq. (3) with $x=1$. Upon rearranging Eq. (3) yields:

$$v_i \approx \left(\left[\frac{1}{2} \cdot \log_{10}(w_s) \right] + 1 \right)^{-1} \quad (6)$$

Table 1 includes the pre-calculated v_i and B_{98} values. The estimated RHD and RHE values are shown in Tables 3 and 4, respectively (not bold). v_i has been estimated from Eq. (6), by using the solubility measurements (w_s) and the required thermodynamic data shown in Table 1; all taken from the CRC Handbook of Chemistry and Physics (2006).

2.2.3 The solute molality μ_s as a function of RH and v_i

EQSAM4 applies Eq. (17d) of the companion paper (M2011), which parameterizes the solute molality μ_s [mol(solute)/kg(H₂O)] as a function of v_i and RH. For RH ≤ 98 [%], i.e.:

$$\mu_s = \mu_s^o \cdot \left(\left[\frac{1}{v_i \cdot \mu_s^o \cdot M_w} \cdot \left(\frac{1}{RH} - 1 \right) \right]^{\frac{1}{v_i}} - B_{98} \right) \quad (7)$$

Figure 1 shows the solute molality calculated with Eq. (7) as a function of water activity for major inorganic compounds. Note that the water activity here is equal to the

[Title Page](#)

[Abstract](#)

[Introduction](#)

[Conclusions](#)

[References](#)

[Tables](#)

[Figures](#)

◀

▶

◀

▶

[Back](#)

[Close](#)

[Full Screen / Esc](#)

[Printer-friendly Version](#)

[Interactive Discussion](#)



[Title Page](#)[Abstract](#)[Introduction](#)[Conclusions](#)[References](#)[Tables](#)[Figures](#)[◀](#)[▶](#)[◀](#)[▶](#)[Back](#)[Close](#)[Full Screen / Esc](#)[Printer-friendly Version](#)[Interactive Discussion](#)

RH. The single solute molalities are plotted from the water activity at saturation, i.e. the RHD calculated with Eq. (1), up to $a_w \leq 0.95$. The results are in good agreement with measurement data used by ISORROPIA II (Fountoukis and Nenes, 2007) and EQUISOLV II (Jacobson, 1999).

2.2.4 The activity coefficient γ_s of semi-volatile species as a function of v_i and RH

As outlined in the companion paper (M2011), v_i substitutes activity coefficients for non-volatile solutes that only undergo solid-liquid partitioning. However, to parameterize the gas-liquid or gas-solid partitioning of (semi-)volatile solutes, an empirical relation between the solute molality μ_s and activity coefficient γ_s is assumed as a function of RH and v_i , following Metzger et al. (2002a) and Metzger and Lelieveld (2007):

$$\gamma_s = z_s \cdot \left(\frac{\mu_s^o}{\mu_s} \right)^{0.5} \quad (8)$$

Currently EQSAM4 applies γ_s for only 2 of the approximately 100 compounds, i.e. for NH_4NO_3 where the (empirical) variable $z_s = 0.7$, and NH_4Cl where $z_s = 1.6$. Note that Eq. (8) accounts for a T -dependency, if v_i is determined, e.g. with the bisection method and Eq. (1) using T -dependent RHD and w_s data (as described in Sect. 3 of M2011). γ_s is shown in Fig. (2) as a function of RH for NH_4NO_3 and NH_4Cl at $T = 298.15$ [K]. For NH_4Cl the saturation molality is used throughout the RH range, i.e. $\mu_s(\text{RH}) = \mu_s(\text{RHD})$ is assumed to obtain γ_s with Eq. (8). The parameterized γ_s values are in reasonable agreement with the data used by ISORROPIA II and EQUISOLV II. A detailed evaluation is the subject of the revised publication of Xu et al. (2009, 2011), which presents a comprehensive model inter-comparison between EQSAM4 and EQUISOLV II. In Sect. 3, EQSAM4 is compared with ISORROPIA II and E-AIM.

2.2.5 The aerosol liquid water content (AWC)

The AWC of single solutions, $m_{w(\text{single})}$ [kg/m³(air)], can be obtained for a given solute concentration n_s [mol/m³(air)] if the solute molality μ_s [mol(solute)/kg(H₂O)] is known:

$$m_{w(\text{single})} = n_s / \mu_s \quad (9)$$

- In EQSAM4 μ_s is obtained from Eq. (7) using the pre-calculated solute specific coefficient v_i , so that Eq. (9) can be readily solved if n_s , T and RH are known. Note that in contrast to other approaches, μ_s obtained from Eq. (7) does not depend on the total AWC of the solution, so that the AWC can be treated as a diagnostic property. This simplifies and speeds up calculations, notably for mixed solutions and global modeling applications.

2.3 Mixed solution parameterizations

EQSAM4 solves the gas-liquid-solid partitioning of mixed solutes non-iteratively by applying an additional parameterization using mean values X_i , which are generally calculated from:

$$\bar{X}_{i,j} = \frac{1}{N} \sum_{j=1,N} (X_{i,j}) \quad (10)$$

$X_{i,j}$ is the i -th of $i = 1, \dots, k$ variables of the j -th of $j = 1, \dots, N$ compounds present in the multicomponent solution (e.g. v_i , w_s , B_{98}) and is used in the corresponding single-solute equation.

2.3.1 The mixed solution aerosol water content (MAWC)

- The MAWC, $m_{w(\text{mix})}$ [kg/m³(air)], is obtained from the ZSR-mixing rule (Stokes and Robison, 1966) and calculated from the sum of all partial water masses, obtained from

[Title Page](#)

[Abstract](#)

[Introduction](#)

[Conclusions](#)

[References](#)

[Tables](#)

[Figures](#)

◀

▶

◀

▶

[Back](#)

[Close](#)

[Full Screen / Esc](#)

[Printer-friendly Version](#)

[Interactive Discussion](#)



$$m_{w(\text{mix})} = \sum_{j=1,N} m_{w(\text{single})} \quad (11)$$

2.3.2 The mixed solution RHD

EQSAM4 has an option to consider a mean i.e. mutual RHD (MRHD) for mixed solutions, which is obtained from Eq. (1) by using the required mean values, following Metzger and Lelieveld (2007). The means are calculated from Eq. (10), but consider only the selected compounds that are dissolved (as described in Sect. 2.1):

$$\text{MRHD} = \left(1 + \mu_s^o \cdot M_w \cdot \bar{v}_i \cdot \left[\frac{\bar{\mu}_s^{\text{sat}}}{\mu_s^o} + \bar{B}_{98} \right]^{\bar{v}_i} \right)^{-1} \quad (12)$$

$\bar{\mu}_{s,j}^{\text{sat}} = \frac{1}{N} \sum_{j=1,N} (\mu_{s,j}^{\text{sat}})$ is the approximated saturation molality at the deliquescence

point of the mixed solution, with the mean computed from the saturation molality at the deliquescence point of the single solution of each dissolved compound, i.e. $\mu_{s,j}^{\text{sat}} = \frac{1}{M_{s,j} \cdot (1/w_{s,j} - 1)}$. Note that $\mu_s^o = 1$ [mol(solute)/kg(H₂O)] has the same value as in Eq. (1). EQSAM4 considers all compounds of the mixed solution as aqueous when their RHD is higher than the mean RHD. These compounds with a RHD below

the MRHD are considered as solids. Thus, the lowest RHD of the mixed compounds determines the onset of water uptake. However, since shape or other correction factors are not considered, the values are indicative (measurements are required for validation). EQSAM4 therefore considers per default the same mixed solution MRHD values as used in ISORROPIA II if the composition matches the same pre-defined aqueous salt compositions listed in Table 5 of Fountoukis and Nenes (2007).

[Title Page](#)[Abstract](#)[Introduction](#)[Conclusions](#)[References](#)[Tables](#)[Figures](#)[◀](#)[▶](#)[◀](#)[▶](#)[Back](#)[Close](#)[Full Screen / Esc](#)[Printer-friendly Version](#)[Interactive Discussion](#)

2.3.3 The mixed solution RHE

EQSAM4 also allows to consider a mean RHE (MRHE) for mixed solutions, which is obtained from Eq. (2) by using the required mean values, also following Metzger and Lelieveld (2007):

$$5 \quad \text{MRHE} = 1 - \left(1 + \mu_s^o \cdot M_w \cdot \bar{v}_i \cdot \left[\frac{\bar{\mu}_s^{\text{sat}}}{\mu_s^o} + \bar{B}_{98} \right]^{\bar{v}_i} \right)^{-1} \quad (13)$$

$\bar{\mu}_{s,j}^{\text{sat}} = \frac{1}{N} \sum_{j=1,N} (\mu_{s,j}^{\text{sat}})$ is the approximated saturation molality at the efflorescence point of the mixed solution, with the mean computed from the saturation molality at the efflorescence point of the single solution of each dissolved compound, i.e., $\mu_{s,j}^{\text{sat}} = \frac{(1/w_{s,j} - 1)}{M_{s,j}}$ and $\mu_s^o = 1$ [mol(solute)/kg(H₂O)]. Since shape or other correction factors are not considered, the values are indicative (measurements are required for validation). The mixed solution MRHE values are partially evaluated in the revised publication of Xu et al. (2009, 2011).

2.3.4 The mixed solution activity coefficient $\gamma_{s(\text{mix})}$

The mixed solution activity coefficient $\gamma_{s(\text{mix})}$ is obtained from γ_s by applying domain specific (empirical) coefficients, x and y that alter the γ_s parameterization given by Eq. (8), i.e.:

$$15 \quad \gamma_{s(\text{mix})} = (y \cdot \gamma_s)^x \quad (14)$$

For the two volatile compounds, NH₄NO₃ and NH₄Cl, $y = 1.725$ and $y = 1$, respectively, and the corresponding x values are listed in Table 7. x in Eq. (14) is different from that in Eq. (3) and is determined for certain cation-anion ratios, i.e. mixed solution domains (D1–10), Table 5, which are in turn used to identify certain regimes (R1–6)

[Title Page](#)

[Abstract](#)

[Introduction](#)

[Conclusions](#)

[References](#)

[Tables](#)

[Figures](#)

◀

▶

◀

▶

[Back](#)

[Close](#)

[Full Screen / Esc](#)

[Printer-friendly Version](#)

[Interactive Discussion](#)



listed in Table 6. To parameterize the aqueous uptake of the residual gases (first row of Table 1 and NH₃), the coefficients given in Table 8 are used. To obtain the dissolved fractions of semi-volatile compounds the ion concentrations are multiplied with the activity coefficients during the neutralization step. In principle there are 60 combinations possible, 10 domains listed in Tables 5 and 6 regimes per domain listed in Table 6. However, most combinations are currently not used. Only certain specific combinations of domains and regimes are applied to determine the activity coefficients for NH₄NO₃, NH₄Cl and the residual gases (i.e. first row of Table 1 and NH₃), as shown in Tables 7 and 8, respectively. For the domains D1, D2, D3, D9 no specification according to Table 6 is needed and the following values are used: $x_{\text{NH}_4\text{NO}_3} = 2$ and $x_{\text{NH}_4\text{Cl}} = 6$ for Table 7, and $x = 2$ and $y = 0.25$ for Table 8. Note that Tables 7 and 8 are considered only for the activity coefficient calculation in mixed solutions and that Table 7 is required only for two compounds, while Table 8 becomes relevant only for high RH, i.e. if RH > 90 [%]. Only under these conditions sufficient aerosol water is predicted to allow for the uptake of gases in aqueous solutions. However, at this RH cloud formation is usually assumed over some portion of the grid in GCMs and the uptake of gases is dominated by uptake in cloud droplets.

2.4 Computational algorithm

EQSAM4 solves the gas-liquid-solid partitioning of single and mixed solutes non-iteratively by applying a set of analytical equations through a solution independent and compound specific coefficient, v_i . The analytical equations depend on v_i and RH and have been detailed in M2011. The EQSAM4 model general solution procedure can be subdivided into four main calculation steps as illustrated in Fig. 3, whereby only step three is executed during runtime:

25 1. Model initialization:

(a) At start up the model reads the gas/aerosol input concentrations at the given T and RH.

EQSAM4 model description

S. Metzger et al.

[Title Page](#)[Abstract](#)[Introduction](#)[Conclusions](#)[References](#)[Tables](#)[Figures](#)[◀](#)[▶](#)[◀](#)[▶](#)[Back](#)[Close](#)[Full Screen / Esc](#)[Printer-friendly Version](#)[Interactive Discussion](#)

(b) The model complexity and speed (during runtime) can be controlled by various switches, e.g. compounds can be individually selected to minimize array sizes and the number of internal compound loops.

(c) The compound specific arrays are initialized using the thermodynamic data provided in Table 1 for the selected compounds only.

2. Pre-calculation of T -dependent look-up tables that are accessed during runtime:

(a) At the second step after model start up compound specific properties are pre-calculated and stored in internal look-up tables for a range of temperature $T = 150\text{--}350\text{ [K]}$.

(b) For compounds for which data is available the T -dependency of the RHD values are calculated from Eq. (4) using the T -coefficients provided in Table 2.

(c) For the same compounds, the T -dependent solute solubility measurements, $w_s(T)$ are applied. The $w_s(T)$ values are taken from the CRC Handbook of Chemistry and Physics (2006) for 5 different temperatures in the range $273\text{--}313\text{ [K]}$ with a 10 [K] interval and a linear interpolation in-between, while for all other compounds listed in Table 1 no T -dependency is applied in the standard model set up. However, for test purposes (e.g. sensitivity studies) an internal switch exits to approximate a T -dependency using Eq. (5).

(d) For the compounds listed in Table 2 the solute specific coefficient v_i is determined from Eq. (1) with the bisection method by using the T -dependent w_s and RHD data, while for all other compounds listed in Table 1 v_i is estimated from w_s . The v_i values are shown in Table 1; the values are printed in bold if they are determined using Eq. (1), otherwise, they are approximated using Eq. (6). The B_{98} values are calculated from Eq. (3) and shown in Table 1; they equal w_s when v_i is estimated from Eq. (6).

(e) The RHD and RHE values for all compounds are calculated from Eq. (1) and (2), respectively, using the T -dependent v_i and w_s lookup table data.

EQSAM4 model description

S. Metzger et al.

The RHD and RHE values are shown in Tables 3 and 4, respectively; bold RHD values indicate that the values are equal to those in Table 2 (they have been used to determine v_i). The T -dependency of the bold RHD data is the same as that applied in ISORROPIA II and shown in Fig. 2 of Fountoukis and Nenes (2007). For the default model setup no T -dependency is considered for the RHD values for all other salt compounds listed in Table 1, and no T -dependency is considered for all RHE values due to the lack of available measurements, except if a T -dependency of the solubility is optionally estimated with Eq. (5). The potentially T -dependent, RHD and RHE values are applied during runtime to solve the liquid-solid partitioning.

- (f) In case the user has chosen that the neutralization reaction order is automatically pre-determined during model start up (in the standard model set up), the (optionally all T -dependent) RHD and RHE values of the selected compounds are ranked so that the array indices determine the neutralization reaction order.
- (g) In case the neutralization reaction order is prescribed, a T -independent and predefined and ion specific ranking (see Sect. 2.1) is applied instead during runtime.
- (h) In case the Kelvin-term is considered, the solute molality μ_s is pre-calculated for the upper RH range, $0.98 < \text{RH} < 1.1$, using T -independent v_i values, by solving the complete μ_s equation, i.e. Eq. (17b) of M2011, with v_i determined at $T = 298.15$ [K]. The μ_s values are stored in internal lookup-tables and accessed during runtime. For the lower RH range, $0 < \text{RH} < 0.98$, μ_s is calculated during runtime from Eq. (7).

3. Runtime calculations – gas/liquid/solid aerosol equilibrium partitioning:

- (a) The look-up tables the RHD, RHE, v_i and potentially μ_s values are assigned to local arrays for the actual temperature and run-time arrays are initialized.



EQSAM4 model description

S. Metzger et al.

- (b) All RH -dependent solute properties are calculated during runtime for a given RH and T for the selected compounds; i.e. the solute molality μ_s is calculated for the lower RH range, $0 < RH < 0.98$ from Eq. (7). Subsequently, μ_s is used by Eq. (8) to obtain the activity coefficient γ_s for the two volatile compounds, NH_4NO_3 and NH_4Cl , and for the gases that are considered for uptake in aqueous solutions, i.e. all compounds in the first row of Table 1 and NH_3 .
- (c) The neutralization reactions are solved and salt compounds are calculated from the neutralization of input cation and anion concentrations, with the reaction order either determined automatically, based on the optional T -dependent RHD or RHE values of the selected compounds, or prescribed (and T -independent). The reaction order is set to be automatic in the standard model setup.
- (d) The aerosol water history determines whether the water uptake and the gas/liquid/solid aerosol equilibrium partitioning is calculated for the deliquescence or efflorescence branch of the hysteresis loop of salt compounds: (i) In case the AWC of the previous computation time step is zero (or below a user defined minimum) deliquescence is assumed and the neutralization reaction order is based on the ranking of the pre-calculated RHD values; (ii) Otherwise the pre-calculated RHE reaction order is applied. Alternatively, the neutralization reaction order can be prescribed, but is in this case T -independent.
- (e) Compounds with the lowest solubility precipitate from solution at higher RH , so that these ions are not available for further reactions. For instance, the solubility of calcium sulfate (CaSO_4) is very low ($< 1 [\%]$) which practically leads to precipitation of CaSO_4 at a fractional RH close to 1, i.e. $RHD = 0.9554$ (Table 2). Once CaSO_4 is precipitated from the solution, the corresponding Ca^{2+} and SO_4^{2-} ions are taken from the solution and hence not available for further neutralization reactions. Then, from the remaining ion concentrations, the following salt compounds are formed and the non-neutralized “free” ions are computed. This procedure is repeated for all selected compounds, which



EQSAM4 model description

S. Metzger et al.

[Title Page](#)[Abstract](#)[Introduction](#)[Conclusions](#)[References](#)[Tables](#)[Figures](#)[◀](#)[▶](#)[◀](#)[▶](#)[Back](#)[Close](#)[Full Screen / Esc](#)[Printer-friendly Version](#)[Interactive Discussion](#)

are kept in the aqueous phase at this stage.

- (f) Bi-salts are specially treated to account e.g. for the fact that sulfate is preferentially neutralized compared to other anions such as nitrates and chlorides, because it is a stronger acid. This is inherent in the internal ranking of indices of the neutralization reaction order.
- (g) For the two volatile salts, NH_4NO_3 and NH_4Cl , activity coefficients are considered for the compound neutralization, and the T -dependent equilibrium constants (same values as in ISORROPIA II and listed in Table 2 of Fountoukis and Nenes, 2007) are applied in the default model set up (these can be switched off for sensitivity tests). All other salt compounds are treated as non-volatile, and equilibrium constants and activity coefficients are not required (the solubility and v_i act as a substitute). Non-volatile compounds remain in the particulate phase independent of the solute concentration, whereby the liquid/solid partitioning is determined by the solute solubility (through RHD or RHE). Since the water mass is proportional to the solute mass (at a given T and RH), additional activity coefficients are not needed for non-volatile compounds; instead, the solubility and v_i are used (see M2011 for details). For (semi-) volatile compounds, which can be driven out of the aerosol into the gas phase, an additional gas-aerosol interaction parameter (activity coefficient) is needed, which we determine similarly to the traditional activity coefficient, γ_s , through a parameterization given by Eq. (8) for single solute solutions, and Eq. (14) for mixed solutions, with the corresponding exponents given in Table 7 for NH_4NO_3 and NH_4Cl .
- (h) Based on the AWC history, the liquid-solid partitioning is calculated using either the RHD or RHE values, whereby all compounds are assumed to be completely precipitated if the RH is below the compound T -dependent RHD or RHE value in case of single solute solutions. The salt compound is removed from the aqueous phase and assumed to be pure solid. In mixed solutions, a solid and liquid phase can co-exist in case compounds have

different RHD or RHE values.

- (i) For salt compounds present in a mixed solution, MRHD and MRHE values are applied; based on Eqs. (12) and (13), respectively. Optionally, the so-called mutual relative humidity of deliquescence (MRHD) values used in ISORROPIA II can be used, if the composition matches the same pre-defined aqueous salt compositions listed in Table 5 of Fountoukis and Nenes (2007); MRHE values are not available. EQSAM4 always applies the lowest RHD (or RHE) value of the compounds present in the solution, e.g. in case the MRHD (or MRHE) value is higher.
- (j) The residual gases and acids (first row of Table 1 and NH₃) are computed from the remaining, i.e. non-neutralized “free” cations and anions. Phosphoric and sulfuric acid can optionally be assumed to remain in the aerosol phase, due to their very low vapor pressures.
- (k) The aerosol liquid water content of single solutes (AWC) and mixed solutions (MAWC) is computed from Eqs. (9) and (11), respectively, for all selected compounds dissolved in the aqueous phase, i.e. when the RHD (or RHE) value is below the actual RH.
- (l) The H⁺ concentration and the pH of the solution is calculated from the MAWC, assuming electroneutrality and accounting for the auto-dissociation of water.
- (m) The uptake of the gases (first row of Table 1 and NH₃) by aqueous solutions is parameterized using Eq. (14) and the corresponding coefficients given in Table 8.
- (n) Non-electrolyte solutes (last row of Table 1) are, except ammonia (NH₃), not directly considered for the determination of the reaction order, nor are they assumed to be involved in neutralization or other reactions. However, they contribute to the aerosol mass, and as long as they remain hydrated also to

EQSAM4 model description

S. Metzger et al.

[Title Page](#)[Abstract](#)[Introduction](#)[Conclusions](#)[References](#)[Tables](#)[Figures](#)[◀](#)[▶](#)[◀](#)[▶](#)[Back](#)[Close](#)[Full Screen / Esc](#)[Printer-friendly Version](#)[Interactive Discussion](#)

EQSAM4 model description

S. Metzger et al.

[Title Page](#)[Abstract](#)[Introduction](#)[Conclusions](#)[References](#)[Tables](#)[Figures](#)[◀](#)[▶](#)[◀](#)[▶](#)[Back](#)[Close](#)[Full Screen / Esc](#)[Printer-friendly Version](#)[Interactive Discussion](#)

the aerosol water mass, and thus can effect the overall aerosol hygroscopic growth.

4. Diagnostic output calculations:

(a) Various aerosol properties can be stored for diagnostic purposes, such as the

solution $pH = -\log \sum_{j=1}^I (n_{s+}/m_w)$, and the ionic strength of binary and mixed

solutions $Z = 0.5 \times (Z_{s+} + Z_{s-}) / m_w$, with $Z_{s+} = \sum_{j=1}^I z_{s+}^{v_s^+}$ and $Z_{s-} = \sum_{j=1}^I z_{s-}^{v_s^-}$ the

total charge of cations and anions, respectively. Aerosol properties such as mass and number of moles, and the associated water mass are stored for each compound listed in Table 2 for each phase (gas, aqueous, solid). Additionally, the total particulate matter (PM), including solids and ions, can

be expressed as the total number of moles, $PM = \sum_{j=1}^I n_s + \sum_{j=1}^I n_s$, the total mass,

$PM_t = \sum_{j=1}^I n_s M_s + \sum_{j=1}^I n_s M_s$, and the total dry mass $PM_s = \sum_{j=1}^I n_s M_s$, whereby

mass and water fractions of all individual compounds are summed, optionally in different units (mol, μmol , or nmol).

5

10

15

3 Model applications

In this section we apply EQSAM4 to solve the gas-liquid-solid partitioning for various single solute and mixed solution modeling examples, including results of box model and global modeling applications. We focus on the RHD/RHE based water uptake of atmospheric aerosols, as this is a key process in atmospheric chemistry and climate modeling studies.

3.1 Box model comparison

We apply v_i to solve the gas-liquid-solid partitioning with EQSAM4 using Eqs. (1–14). The results in this sub-section are all based on v_i obtained from RHD measurements and compared to reference calculations of E-AIM and ISORROPIA II. For comparison, 5 results based on v_i estimated from Eq. (6) are included (label EQSAM4-Eq6).

3.1.1 Fixed solute concentrations: EQSAM4 vs. E-AIM and ISORROPIA II

Figure 4 present results of a box model inter-comparison using EQSAM4 and the thermodynamic reference model, E-AIM (Wexler and Clegg, 2002; <http://www.aim.env.uea.ac.uk/aim/aim.php>), and the thermodynamic model ISORROPIA II (Fountoukis and Nenes, 2007). ISORROPIA II is included in our global chemistry climate model EMAC (Pringle et al., 2010) – a comparison is given in the next section. The results in this section are based on the same RHD and MRHD values as used in ISORROPIA II, and the coefficients listed in Tables 7 and 8 have been applied to parameterize the mixed solution activity coefficient of volatile compounds with Eq. (14), i.e. NH_4NO_3 , NH_4Cl , and the aqueous uptake of residual gases NH_3 , HNO_3 and HCl .
10
15

Figure 4a–e shows box model results for the gas/liquid/solid aerosol equilibrium partitioning of various single salt solutions, and Fig. 4g–h shows the results of two corresponding mixed solutions. The solute concentrations were fixed to 1 [$\mu\text{mol}/\text{m}^3$]. The aerosol water and the RHD predicted by EQSAM4 compare relatively well with the predictions of E-AIM and ISORROPIA II for all salt solutions, although minor discrepancies occur. The main discrepancy between EQSAM4 and ISORROPIA II occurs at the phase transitions near the mutual RHD for the mixed solution case (h), which includes NH_4Cl , although the same MRHD values as used in ISORROPIA II have been applied for the mixed solution cases. The reason is that for this particular case ISORROPIA II 20 does not predict NH_4Cl to be present in the mutual deliquescence RH regime, while it is the case for EQSAM4 and E-AIM. Near the upper end of the RH range, i.e. at high RH above 95 [%], the EQSAM4 aerosol water prediction starts to deviate from those 25

[Title Page](#)

[Abstract](#)

[Introduction](#)

[Conclusions](#)

[References](#)

[Tables](#)

[Figures](#)

[◀](#)

[▶](#)

[◀](#)

[▶](#)

[Back](#)

[Close](#)

[Full Screen / Esc](#)

[Printer-friendly Version](#)

[Interactive Discussion](#)



EQSAM4 model description

S. Metzger et al.

[Title Page](#)[Abstract](#)[Introduction](#)[Conclusions](#)[References](#)[Tables](#)[Figures](#)[◀](#)[▶](#)[◀](#)[▶](#)[Back](#)[Close](#)[Full Screen / Esc](#)[Printer-friendly Version](#)[Interactive Discussion](#)

of E-AIM and ISORROPIA II, since the applied parameterization of solute molality, Eq. (7), becomes invalid. For cases with high RH values, the solute molality including the Kelvin-term should be used (see M2011). Nevertheless, the aerosol water uptake agrees well with the reference calculations, even if v_i is estimated from Eq. (6), except for case (f), i.e. NH_4HSO_4 , where the simplified v_i estimation works less well. For compounds that do not dissociate completely, e.g. bi-sulfates (case (f)), this simplified estimation leads to relatively larger errors compared to compounds that practically dissociate completely, e.g. NaCl; i.e. comparing case (a) and (f). For a comprehensive model evaluation we refer to the revised publication of Xu et al. (2009, 2011), which complements this work. Next, we continue with mixed solution box modeling applications using observations following Metzger et al. (2006).

3.1.2 MINOS campaign: EQSAM4 vs. ISORROPIA II

To extend our model inter-comparison for mixed solutions, we apply EQSAM4 to real cases, i.e. measurements obtained from MINOS (Mediterranean INtensive Oxidant Study) in Crete in the period 27 July to 25 August 2001 following Metzger et al. (2006). For a general description of the measurements and the modeling set-up we refer to that article. Here, we compare EQSAM4 with ISORROPIA II and apply both models with the same level of complexity, considering the ammonium/sulfate/nitrate/chloride/sodium/calcium/magnesium/potassium/water system.

The EQSAM4 results in this section are based on the same RHD values as used in ISORROPIA II, while the MRHD values have been obtained from Eq. (12), and only the default cases with coefficients as in C0 of Table 7, i.e. $x = 2$ and $x = 6$ for the two volatile compounds, NH_4NO_3 and NH_4Cl , respectively, have been applied to parameterize the mixed solution activity coefficient with Eq. (14) for all mixed solution cases (time steps, i.e. data points). The aqueous uptake of residual gases NH_3 , HNO_3 and HCl is negligible since total aerosol liquid water content (AWC) is predicted to be rather low in the considered observation period, due the relatively high temperature and low relative humidity; $T > 295\text{[K]}$ and $\text{RH} < 90\text{[%]}$, see panels (g) and (h) in Fig. 6 for T and

RH, and respectively panels (a) in Figs. 5 and 6 for the total AWC of the aerosol fine and coarse mode. Figure 5 shows 4-weekly time series of model calculated mixed solution properties for the aerosol fine mode; observations are included where available. Figure 6 also shows the coarse mode results. The results of EQSAM4 and ISORROPIA II are close for all cases when v_i is determined from the compound's RHD. But even if v_i is estimated from Eq. (6) (labeled EQSAM4-Eq6) the results are rather close to ISORROPIA II. The relatively largest deviations occur for the aerosol water mass predictions and the liquid-solid partitioning.

Both models predict the same amounts of residual gases, NH_3 , HNO_3 and HCl and a similar amount of the corresponding aerosol ammonium and nitrate in both the fine and coarse mode. Also the calculations of the low aerosol nitrate concentrations are similar, although quite sensitive to the activity coefficient of ammonium nitrate, but both models tend to overestimate the NO_3^- and Cl^- in the coarse mode compared to the observations, since the semi-volatile inorganic matter tends to be not in equilibrium. And the models do not necessarily need to be in agreement with ammonia and the observations of fine mode ammonium. The reason is that organic acids are omitted in this comparison because ISORROPIA II does not include them. Metzger et al. (2006) showed that the presence of ammonium in the aerosol phase could be dependent on the presence of organic acids (e.g. from biomass burning) in cases where alkali-cations (e.g. mineral dust) are present in excess of inorganic acids, so that a consistent inclusion of alkaline cations and organic acids seems to be important for the gas/aerosol partitioning of reactive nitrogen compounds for both fine and coarse mode particles. In contrast to the cation ammonium, the anion nitrate is less affected in the fine mode than in the coarse mode, so that the aerosol nitrate predictions of EQSAM4 are closer to the observations for these cases.

3.2 Global model application with EMAC

To test the applicability of EQSAM4 in global modeling, we have applied EQSAM4 within our global chemistry climate model EMAC, with the setup exactly as in Pringle

EQSAM4 model description

S. Metzger et al.

[Title Page](#)

[Abstract](#)

[Introduction](#)

[Conclusions](#)

[References](#)

[Tables](#)

[Figures](#)

◀

▶

◀

▶

[Back](#)

[Close](#)

[Full Screen / Esc](#)

[Printer-friendly Version](#)

[Interactive Discussion](#)



et al. (2010). We therefore refrain from further model description and refer instead to that article. Figures 7 and 8 complement their Figs. 14 and 15, showing the same results for EQSAM4 instead for ISORROPIA II (both gas-aerosol partitioning models are embedded within EMAC/GMXe and applied exactly the same). Figure 7 compares the 5 EQSAM4 based results with data collected by AEROCE. Maps show the surface concentration of nitrate (top) and sulfate (bottom) for the year 2002; the observations are overplotted (squares). Scatter plots show the comparison of the EQSAM4 model vs. AEROCE data for nitrate (top) and sulfate (bottom). Figure 8 (top) additionally shows the annual mean AOD modeled with GMXe/EQSAM4 for the year 2001; over-plotted 10 are annual mean measurements from the AERONET network (2001), and a summary of the comparison between GMXe using EQSAM4 and AERONET is given in the left bottom panel, while the right bottom panel shows the annual mean AOD from MODIS for the year 2001. Both figures are similar to the ISORROPIA II based ones shown in Pringle et al. (2010). We only include these results for the purpose of a consistent 15 model inter-comparison between EQSAM4 and ISORROPIA II within EMAC. For a comprehensive AOD evaluation a coupling of the gas-aerosol partitioning module (here EQSAM4 or ISORROPIA II) with the module that calculates the size-dependent aerosol dynamics (GMXe), following e.g. Feng and Penner (2007), is required. A further development is foreseen.

20 4 Conclusions

Version 4 of the EQuilibrium Simplified Aerosol Model (EQSAM4), which is part of our 25 aerosol chemistry-microphysics module (GMXe) and chemistry-climate model (EMAC), is described and evaluated. We focus on the RHD based water uptake of atmospheric aerosols, e.g. important for calculations of the aerosol optical depth (AOD). The key equations on which EQSAM4 builds are detailed in M2011 (companion paper) and based on a solute specific coefficient v_i . To demonstrate the applicability of EQSAM4, we have given some examples; starting from computations based on the key equations,

EQSAM4 model description

S. Metzger et al.

[Title Page](#)

[Abstract](#)

[Introduction](#)

[Conclusions](#)

[References](#)

[Tables](#)

[Figures](#)

◀

▶

◀

▶

[Back](#)

[Close](#)

[Full Screen / Esc](#)

[Printer-friendly Version](#)

[Interactive Discussion](#)



EQSAM4 model description

S. Metzger et al.

[Title Page](#)[Abstract](#)[Introduction](#)[Conclusions](#)[References](#)[Tables](#)[Figures](#)[◀](#)[▶](#)[◀](#)[▶](#)[Back](#)[Close](#)[Full Screen / Esc](#)[Printer-friendly Version](#)[Interactive Discussion](#)

to box and global modeling. It appears that the v_i concept can be applied to solve the gas-liquid-solid partitioning of single solute or mixed solutions and thus the RHD/RHE based water uptake of atmospheric aerosols. The results of EQSAM4 closely agree with the results of the thermodynamic reference model E-AIM and also with ISORROPIA II for various single and mixed salt solutions. A more comprehensive box-model comparison is the subject of a revised publication (Xu et al., 2009, 2011). Our box model results are supported by global modeling applications and a comparison with measurements and with results of ISORROPIA II, as presented earlier following Pringle et al. (2010). Our results indicate that the revised EQSAM model provides a valid parameterization for global modeling.

Acknowledgements. This work was supported by the CIRCE Integrated Project – Climate Change and Impact Research: the Mediterranean Environment (<http://www.circeproject.eu/>) and supported by the European Commission's Sixth Framework Program, Sustainable Development, Global Change and Ecosystems, Project No. 036961. We are grateful to the ERC for support of the C8 project. LX and JEP are grateful for the support of the NASA Glory Science Team under grant number NNX08AL83G as well as that from NASA JPL under contract number NM0710973. LX is grateful for the support by the Max Planck Society. We thank T. Nenes for kindly providing the ISORROPIA II source code and S. L. Clegg and A. S. Wexler for the www version of E-AIM. We thank K. Pringle and H. Tost for their support with the ongoing model development of EQSAM/GMXe.

References

- Adams, P. J., Seinfeld, J. H., Koch, D., Mickley, L., and Jacob, D.: General circulation model assessment of direct radiative forcing by the sulfate-nitrate-ammonium-water inorganic aerosol system, *J. Geophys. Res.*, 106, 1097–1112, doi:10.1029/2000JD900512, 2001.
- Amundson, N. R., Caboussat, A., He, J. W., Martynenko, A. V., Savarin, V. B., Seinfeld, J. H., and Yoo, K. Y.: A new inorganic atmospheric aerosol phase equilibrium model (UHAERO), *Atmos. Chem. Phys.*, 6, 975–992, doi:10.5194/acp-6-975-2006, 2006.
- Ansari, A. S. and Pandis, S. N.: Prediction of multicomponent inorganic atmospheric aerosol behavior, *Atmos. Environ.*, 33, 745–757, 1999.

- Ansari, A. S. and Pandis, S. N.: The effect of metastable equilibrium states on the partitioning of nitrate between the gas and aerosol phases, *Atmos. Environ.*, 34, 157–168, 2000.
- Bassett, M., and Seinfeld, J. H.: Atmospheric equilibrium model of sulfate and nitrate aerosol, *Atmos. Environ.*, 17, 2237–2252, 1983.
- 5 Bassett, M., and Seinfeld, J. H.: Atmospheric equilibrium model of sulfate and nitrate aerosols – II. particle size analysis, *Atmos. Environ.*, 18, 1163–1170, 1984.
- Bauer, S. E., Mishchenko, M. I., Lacis, A. A., Zhang, S., Perlitz, J., and Metzger, S. M.: Do sulfate and nitrate coatings on mineral dust have important effects on radiative properties and climate modeling?, *J. Geophys. Res.*, 112, D06307, doi:10.1029/2005JD006977, 2007a.
- 10 Bauer, S. E., Koch, D., Unger, N., Metzger, S. M., Shindell, D. T., and Streets, D. G.: Nitrate aerosols today and in 2030: a global simulation including aerosols and tropospheric ozone, *Atmos. Chem. Phys.*, 7, 5043–5059, doi:10.5194/acp-7-5043-2007, 2007b.
- Binkowski, F. and Shankar, U.: The regional particulate matter model, 1: model description and preliminary results, *J. Geophys. Res.*, 100, 26191–26209, 1995.
- 15 Brühl, C., Lelieveld, J., Crutzen, P. J., and Tost, H.: The role of carbonyl sulphide as a source of stratospheric sulphate aerosol and its impact on climate, *Atmos. Chem. Phys. Discuss.*, 11, 20823–20854, doi:10.5194/acpd-11-20823-2011, 2011.
- Chemical Rubber Company (CRC): Handbook of Chemistry and Physics, 86th Edition, Taylor and Francis Group LLC, 2004–2005, CD-ROM version 2006.
- 20 Feng, Y. and Penner, J. E.: Global modeling of nitrate and ammonium: Interaction of aerosols and tropospheric chemistry, *J. Geophys. Res.*, 112, D01304, doi:10.1029/2005JD006404, 2007.
- Fountoukis, C. and Nenes, A.: ISORROPIA II: a computationally efficient thermodynamic equilibrium model for K^+ – Ca^{2+} – Mg^{2+} – NH_4^+ – Na^+ – SO_4^{2-} – NO_3^- – Cl^- – H_2O aerosols, *Atmos. Chem. Phys.*, 7, 4639–4659, doi:10.5194/acp-7-4639-2007, 2007.
- 25 Hofmeister, F.: Zur Lehre von der Wirkung der Salze, *Arch. Exp. Pathol. Pharmakol.*, (Leipzig) 24 (1888) 247–260; translated in: Zur Lehre von der Wirkung der Salze (about the science of the effect of salts: Franz Hofmeister's historical papers, edited by: Kunz, W., Henle, J., and Ninham, B. W., *Curr. Opin. Coll. Interface Sci.*, 9, 19–37, 2004.
- 30 Jacobson, M., Tabazadeh, A., and Turco, R.: Simulating equilibrium within aerosols and non equilibrium between gases and aerosols, *J. Geophys. Res.*, 101 (D4), 9079–9091, 1996.
- Jacobson, M. Z.: Global direct radiative forcing due to multicomponent anthropogenic and natural aerosols, *J. Geophys. Res.*, 106, 1551–1568, 2001.

EQSAM4 model description

S. Metzger et al.

[Title Page](#)[Abstract](#)[Introduction](#)[Conclusions](#)[References](#)[Tables](#)[Figures](#)[◀](#)[▶](#)[◀](#)[▶](#)[Back](#)[Close](#)[Full Screen / Esc](#)[Printer-friendly Version](#)[Interactive Discussion](#)

EQSAM4 model description

S. Metzger et al.

[Title Page](#)[Abstract](#)[Introduction](#)[Conclusions](#)[References](#)[Tables](#)[Figures](#)[◀](#)[▶](#)[◀](#)[▶](#)[Back](#)[Close](#)[Full Screen / Esc](#)[Printer-friendly Version](#)[Interactive Discussion](#)

- Jacobson, M.: Simulating equilibrium within aerosols and non equilibrium between gases and aerosols, *Atmos. Environ.*, 30, 3635–3649, 1999.
- Jacobson, M. Z.: Global direct radiative forcing due to multicomponent anthropogenic and natural aerosols, *J. Geophys. Res.*, 106, 1551–1568, 2001.
- 5 Kim, Y. P. and Seinfeld, J. H.: Atmospheric gas-aerosol equilibrium III. thermodynamics of crustal elements Ca^{2+} – K^+ – Mg^{2+} , *Aerosol Sci. Technol.*, 19, 182–198, 1995
- Kim, Y. P., Seinfeld, J. H., and Saxena, P.: Atmospheric gas-aerosol equilibrium I. thermodynamic model, *Aerosol Sci. Technol.*, 19, 157–181, 1993a.
- 10 Kim, Y. P., Seinfeld, J. H., and Saxena, P.: Atmospheric gas-aerosol equilibrium II. Analysis of common approximations and activity coefficient calculation methods, *Aerosol Sci. Technol.*, 19, 182–198, 1993b.
- Lauer, A., Hendricks, J., Ackermann, I., Schell, B., Hass, H., and Metzger, S.: Simulating aerosol microphysics with the ECHAM/MADE GCM – Part I: Model description and comparison with observations, *Atmos. Chem. Phys.*, 5, 3251–3276, doi:10.5194/acp-5-3251-2005, 2005.
- 15 Liao, H., Adams, P. J., Chung, S. H., Seinfeld, J. H., Mickley, L. J., and Jacob, D. J.: Interactions between tropospheric chemistry and aerosols in a unified general circulation model, *J. Geophys. Res.*, 108, 4001, doi:10.1029/2001JD001260, 2003.
- Liao, H. and Seinfeld, J. H.: Global impacts of gas-phase chemistry-aerosol interactions 20 on direct radiative forcing by anthropogenic aerosols and ozone, *J. Geophys. Res.*, 110, doi:10.1029/2005JD005907, 2005.
- Liao, H., Chen, W.-T., and Seinfeld, J. H.: Role of climate change in global predictions of future tropospheric ozone and aerosols, *J. Geophys. Res.*, 111, doi:10.1029/2005JD006 852, 2006.
- 25 Luo, C., Zender, C. S., Bian, H., and Metzger, S.: Role of ammonia chemistry and coarse mode aerosols in global climatological inorganic aerosol distributions, *Atmos. Environ.*, 41, 2510–2533, 2007.
- Makar, P. A., Bouchet, V. S., and Nenes, A.: Inorganic chemistry calculations using HETV – 30 a vectorized solver for the SO_4^{2-} – NO_3^- – NH_4^+ system based on the ISORROPIA algorithms, *Atmos. Environ.*, 37, 2279–2294, 2003.
- Martin, S. T., Hung, H.-M., Park, R. J., Jacob, D. J., Spurr, R. J. D., Chance, K. V., and Chin, M.: Effects of the physical state of tropospheric ammonium-sulfate-nitrate particles on global aerosol direct radiative forcing, *Atmos. Chem. Phys.*, 4, 183–214, doi:10.5194/acp-4-183-

2004, 2004.

Meng, Z. Y., Seinfeld, J. H., Saxena, P., and Kim, Y. P.: Atmospheric gas-aerosol equilibrium IV. thermodynamics of carbonates, *Aerosol Sci. Technol.*, 23, 517, 131–154, 1995.

Meng, Z. and Seinfeld, J. H.: Time scales to achieve atmospheric gas/aerosol equilibrium for volatile species, *Atmos. Environ.*, 30, 2889–2900, 1996.

Metzger, S. M.: Gas/Aerosol Partitioning: A simplified Method for Global Modeling, Ph.D. Thesis, University Utrecht, The Netherlands, ISBN:90-393-2510-3, <http://igitur-archive.library.uu.nl/dissertations/1930853/inhoud.htm>, 2000.

Metzger, S. M., Dentener, F. J., Lelieveld, J., and Pandis, S. N.: Gas/aerosol partitioning I: A computationally efficient model, *J. Geophys. Res.*, 107(D16), doi:10.1029/2001JD001102, 2002a.

Metzger, S. M., Dentener, F. J., Jeuken, A., Krol, M., and Lelieveld, J.: Gas/aerosol partitioning II: global modeling results, *J. Geo- phys. Res.*, 107(D16), 4313, doi:10.1029/2001JD001103, 2002b.

Metzger, S., Mihalopoulos, N., and Lelieveld, J.: Importance of mineral cations and organics in gas-aerosol partitioning of reactive nitrogen compounds: case study based on MINOS results, *Atmos. Chem. Phys.*, 6, 2549–2567, doi:10.5194/acp-6-2549-2006, 2006.

Metzger, S. and Lelieveld, J.: Reformulating atmospheric aerosol thermodynamics and hygroscopic growth into fog, haze and clouds, *Atmos. Chem. Phys.*, 7, 3163–3193, doi:10.5194/acp-7-3163-2007, 2007.

Metzger, S., Steil, B., Penner, J. E., Xu, L., and Lelieveld, J.: Derivation of the stoichiometric coefficient of water (v_w) to account for water uptake by atmospheric aerosols, *Atmos. Chem. Phys. Discuss.*, 10, 8165–8188, doi:10.5194/acpd-10-8165-2010, 2010.

Metzger, S., Steil, B., Xu, L., Penner, J. E., and Lelieveld, J.: Aerosol hygroscopic growth parameterization based on a solute specific coefficient, *Atmos. Chem. Phys. Discuss.*, 11, 24813–24855, doi:10.5194/acpd-11-24813-2011, 2011.

Myhre, G., Grini, A., and Metzger, S.: Modelling of nitrate and ammonium-containing aerosols in presence of sea salt, *Atmos. Chem. Phys.*, 6, 4809–4821, doi:10.5194/acp-6-4809-2006, 2006.

Nenes, A., Pilinis, C., and Pandis, S. N.: ISORROPIA: A new thermodynamic model for multi-phase multicomponent inorganic aerosols, *Aquat. Geochem.*, 4, 123–152, 1998.

Nenes, A., Pilinis, C., and Pandis, S. N.: Continued development and testing of a new thermodynamic aerosol module for urban and regional air quality models, *Atmos. Environ.*, 33,

EQSAM4 model description

S. Metzger et al.

[Title Page](#)

[Abstract](#)

[Introduction](#)

[Conclusions](#)

[References](#)

[Tables](#)

[Figures](#)

◀

▶

◀

▶

[Back](#)

[Close](#)

[Full Screen / Esc](#)

[Printer-friendly Version](#)

[Interactive Discussion](#)



1553–1560, 1999.

Pilinis, C. and Seinfeld, J.: Continued development of a general equilibrium model for inorganic multicomponent atmospheric aerosols, *Atmos. Environ.*, 21, 2453–2466, 1987.

Pilinis, C., Capaldo, K. P., Nenes, A., and Pandis, S. N.: MADM-A new multicomponent aerosol dynamics model, *Aerosol Sci. Technol.*, 32, 482–502, 2000.

Pringle, K. J., Tost, H., Metzger, S., Steil, B., Giannadaki, D., Nenes, A., Fountoukis, C., Stier, P., Vignati, E., and Lelieveld, J.: Corrigendum to “Description and evaluation of GMXe: a new aerosol submodel for global simulations (v1)” published in *Geosci. Model Dev.*, 3, 391–412, 2010, *Geosci. Model Dev.*, 3, 413–413, doi:10.5194/gmd-3-413-2010, 2010.

Pozzer, A., de Meij, A., Pringle, K. J., Tost, H., Doering, U. M., van Aardenne, J., and Lelieveld, J.: Aerosol simulation applying high resolution anthropogenic emissions with the EMAC chemistry-climate model, *Atmos. Chem. Phys. Discuss.*, 11, 25205–25261, doi:10.5194/acpd-11-25205-2011, 2011.

Rodriguez, M. A. and Dabdub, D.: IMAGES-SCAPE2: A modeling study of size and chemically resolved aerosol thermodynamics in a global chemical transport model, *J. Geophys. Res.*, 109, D02203, doi:10.1029/2003JD003639, 2004.

Saxena, P., Hudishevskyj, A. B., Seigneur, C., and Seinfeld, J. H.: A comparative study of equilibrium approaches to the chemical characterization of secondary aerosols, *Atmos. Environ.*, 20, 1471–1483, 1986.

Stokes, R. H. and Robinson, R. A.: Interactions in aqueous nonelectrolyte solutions. I. Solute solvent equilibria, *J. Phys. Chem.*, 70, 2126–2130, 1966.

Trebs, I., Metzger, S., Meixner, F. X., Helas, G., Hoffer, A., Andreae, M. O., Moura, M. A. L., da Silva, R. S., Slanina, J., Rudich, Y., Falkovich, A., and Artaxo, P.: The $\text{NH}_4^+ - \text{NO}_3^- - \text{Cl}^- - \text{SO}_2 - \text{H}_2\text{O}$ system and its gas phase precursors at a rural site in the Amazon Basin: How relevant are crustal species and soluble organic compounds?, *J. Geophys. Res.-Atmos.*, 110, D07303, doi:10.1029/2004JD005478, 2005.

Topping, D. O., McFiggans, G. B., and Coe, H.: A curved multi-component aerosol hygroscopicity model framework: Part 1 – Inorganic compounds, *Atmos. Chem. Phys.*, 5, 1205–1222, doi:10.5194/acp-5-1205-2005, 2005a.

Topping, D. O., McFiggans, G. B., and Coe, H.: A curved multi-component aerosol hygroscopicity model framework: Part 2 – Including organic compounds, *Atmos. Chem. Phys.*, 5, 1223–1242, doi:10.5194/acp-5-1223-2005, 2005b.

Tsigaridis, K., Krol, M., Dentener, F. J., Balkanski, Y., Lathière, J., Metzger, S., Hauglustaine,

Discussion Paper | EQSAM4 model description

S. Metzger et al.

[Title Page](#)

[Abstract](#)

[Introduction](#)

[Conclusions](#)

[References](#)

[Tables](#)

[Figures](#)

◀

▶

◀

▶

[Back](#)

[Close](#)

[Full Screen / Esc](#)

[Printer-friendly Version](#)

[Interactive Discussion](#)



EQSAM4 model description

S. Metzger et al.

[Title Page](#)[Abstract](#)[Introduction](#)[Conclusions](#)[References](#)[Tables](#)[Figures](#)[|◀](#)[▶|](#)[◀](#)[▶](#)[Back](#)[Close](#)[Full Screen / Esc](#)[Printer-friendly Version](#)[Interactive Discussion](#)

Table 1a. EQSAM4 compounds and data.

Anions→ Cations↓	Phosphate PO_4^{3-}	Sulfate SO_4^{2-}	Hydrogen Sulfate HSO_4^-	Nitrate NO_3^-	Chloride Cl^-	Bromide Br^-	Iodide I^-
	H_3PO_4	H_2SO_4	---	HNO_3	HCl	HBr	HI
Hydrogen H^+	97.995 4	84.57 0.8457	- 1.0378	98.08 0.7000	70 1.0840	1.83 -	- -
				63.01 2	25 0.250	1.51 1.4307	3 2
				3 2	36.46 0.15	15 1.701	49.81 2
				80.91 2	25 0.250	3.307 1.4307	127.9 2
				25 2	3.307 0.3000	127.9 1.3540	5.228 1.3540
Ammonium NH_4^+	(NH_4) ₃ $\text{PO}_4 \cdot 3\text{H}_2\text{O}$ 164 4	(NH_4) ₂ SO_4 20 0.2000	NH_4HSO_4 45.11 ^{**} 1.3056	NH_4NO_3 76 2.0845	NH_4Cl 53.49 1.2552	NH_4Br 27.3 ^{**} 1.0519	NH_4I 49.74 1.2552
Sodium Na^+	$\text{Na}_3\text{PO}_4 \cdot 12\text{H}_2\text{O}$ 380.12 4	Na_2SO_4 13.00 0.1300	NaHSO_4 142.0 0.7954	NaNO_3 21.94 0.2927	NaCl 48.7 ^{**} 0.7968	NaBr 58.44 1.0519	NaI 102.9 1.3540
Potassium K^+	K_3PO_4 212.3 4	K_2SO_4 51.46 0.5146	KHSO_4 174.3 1.1686	KNO_3 11.71 ^{**} 0.1171	KCl 2.26 1.3624	KBr 28.39 ^{**} 1.1991	KI 74.55 0.9621
Calcium Ca^{2+}	$\text{Ca}_3(\text{PO}_4)_2$ 310.2 3	CaSO_4 81.71 ^{**} 1.0459	---	$\text{Ca}(\text{NO}_3)_2$ 2.96 0.2937	CaCl_2 58.22 ^{**} 0.9621	CaBr_2 2.5 1.279	CaI_2 111 2
Magnesium Mg^{2+}	$\text{Mg}_3(\text{PO}_4)_2 \cdot 5\text{H}_2\text{O}$ 263 3	MgSO_4 94.88 ^{**} 1.0115	---	$\text{Mg}(\text{NO}_3)_2$ 2.66 0.2020	MgCl_2 59.59 ^{**} 1.9922	MgBr_2 2.3 0.0806	MgI_2 95.21 2.207
Iron(II,III) $\text{Fe}^{2+}, \text{Fe}^{3+}$	$\text{FePO}_4 \cdot 2\text{H}_2\text{O}$ 151 2	$\text{Fe}_2(\text{SO}_4)_3$ 72.25 0.7225	---	$\text{Fe}(\text{NO}_3)_3$ 3.1 0.8148	FeCl_3 45.21 0.4521	FeBr_3 162.2 1.2083	FeI_2 47.7 0.4770
				241.9 4	295.6 4	309.7 1.192	7.0 4
				241.9 4	295.6 4	309.7 0.8198	7.0 1.0451
				241.9 4	295.6 4	309.7 0.07	7.0 1.7954

Formula

 M_s = solute molar mass [g/mol] M_s W_s P_s V_s = solute stoichiometric constant, complete dissociation [-] B_{98} = B-term [-], Eq.(3) with $x = 1$ in case v_i not indicated bold V_i = solute specific coefficient [-], bold v_i = Eq.(1), else = Eq.(6) M_s, W_s, P_s data from CRC-Handbook of Chemistry and Physics, 85th Edition, 2004-2005.The solubility W_s is based on measurements that correspond to aqueous solutions at $T=25^\circ\text{C}$, except noted: $\approx 15^\circ\text{C}$, $\approx 20^\circ\text{C}$.Ms account for the dry mass excluding any mass of hydration. Solvent (water) molar mass $M_w = 18.015$ [g/mol], density of the solution P [g/mL]. For a compound with low solubility ($-W_s < 1\%$) the error from approximating the density is generally less than the uncertainty in the experimental solubility measurement. v_i , if bold, is determined from the compound's RHD by solving Eq. (1) with the bisection method using the solubility and RHD measurements at $T=25^\circ\text{C}$.**EQSAM4 model description**

S. Metzger et al.

Title Page

Abstract

Introduction

Conclusions

References

Tables

Figures

◀

▶

◀

▶

Back

Close

Full Screen / Esc

Printer-friendly Version

Interactive Discussion



EQSAM4 model description

S. Metzger et al.

Table 1b. Continued.

Anions→ Cations↓	Carbonate CO_3^{2-}			Hydrogen Carbonate HCO_3^-			Hydroxide OH^-			Formate CHO_2^-			Acetate $\text{C}_2\text{H}_3\text{O}_2^-$			Oxalate $\text{C}_2\text{O}_4^{2-}$			Citrate $\text{C}_6\text{H}_5\text{O}_7^{3-}$		
	H_2CO_3			---			H_2O			CH_2O_2			$\text{C}_2\text{H}_4\text{O}_2$			$\text{C}_2\text{H}_5\text{O}_4$			$\text{C}_6\text{H}_8\text{O}_7$		
Hydrogen H^+	62.025 3	1.150 0.015	- 1.7954	- -	- -	- -	18015 2	100 0.000	0.997 1.0000	46.03 2	68 0.6800	1.22 1.0914	60.05 2	23 0.2300	1.045 1.4687	90.04 3	8.69' 0.0869	1.9 1.7954	192.1 4	59' 0.59	1.665 1.1294
Ammonium NH_4^+	(NH_4) ₂ CO_3 96.086 3	50.00' 0.50	- 1.1772	79.06 2	19.87 1.5406	1.586 2	35.05 1.0000	100 1	- 2	63.06 0.5885	58.85 1.1301	1.27 2	77.08 0.5968	59.68 1.1262	1.073 3	124.1 0.0494	4.94 1.7954	1.5 4	226.2 0.8618	88.18 1.0281	1.48
Sodium Na^+	Na_2CO_3 105.99 3	23.49 0.2384	2.54 1.4589	84.01 2	9.34 0.0934	2.2 1.7954	40.0 2	50 0.5000	2.13 1.1772	68.01 2	48.69 0.4869	1.92 1.1852	82.03 2	33.51 0.3351	1.528 1.3113	134 3	3.48 0.0348	3.61 1.7954	258.1 4	36.0 0.36	- 1.2851
Potassium K^+	K_2CO_3 138.21 3	52.61 0.5261	22.9 1.1621	100.1 2	25.78 0.2578	2.17 1.4172	56.11 2	54.75 0.5475	2.044 1.1505	84.12 2	76.80' 0.7680	1.91 1.0608	98.14 2	72.9 0.7290	1.57 1.0737	166 3	26.68 0.2668	2.13 1.4023	306.4 4	94.10 0.9410	- 1.0134
Calcium Ca^{2+}	CaCO_3 100.09 2	0.200 0.20	2.83 1.7954	- -	- -	- -	74.09 3	0.26 0.26	2.2 1.7954	130.1 3	14.24' 0.1424	2.02 1.7338	158.2 3	82.87 0.8287	1.5 1.0425	128.1 2	0.4 0.4	2.2 1.7954	498.4 5	96.38 0.9638	- 1.0081
Magnesium Mg^{2+}	MgCO_3 84.314 2	0.220 0.20	3.05 1.7954	- -	- -	- -	58.32 3	0.50 0.50	2.37 1.7954	114 3	87.99 0.8799	- 1.0286	142.4 3	39.61 0.3961	1.5 1.2517	112.3 2	83.91 0.8391	- 1.0396	451 5	95.99 0.9599	- 1.0090
Iron(II,III) $\text{Fe}^{2+}, \text{Fe}^{3+}$	FeCO_3 115.85 2	39.17 0.3917	3.9 1.2555	- -	- -	- -	106.9 4	47.26 0.4726	3.12 1.1944	191 4	45.21' 0.4521	- 1.2083	190.9 4	90.54 0.9054	- 1.0221	375.8 5	95.19 0.9519	- 1.0108	245 2	94.61 0.9461	- 1.0122



Printer-friendly Version

Interactive Discussion

EQSAM4 model description

S. Metzger et al.

Table 1c. Continued.

Solutes	Ammonia		Acetone		Methanol		Ethanol		D-Fructose		D-Mannitol		Sucrose								
	NH ₃	(CH ₃) ₂ CO	CH ₃ OH	CH ₃ CH ₂ OH	C ₆ H ₁₂ O ₆	C ₆ H ₁₄ O ₆	C ₁₂ H ₂₂ O ₁₁														
	17.031	30	0.696	58.08	13	0.785	32.04	100	0.791	46.07	100	0.789	180.2	48	1.6	182.2	15	1.489	342.3	80	1.581
	1	0.30	1.3540	3	0.1300	1.7954	2	1.0	1.0000	3	1.0	1.0000	6	0.4800	1.19	11	1.5E-01	1.7005	11	8.0E-01	1.0509
Solutes	Mercury		Lead		Levoglucosan		Succinic		Fulvic acid												
	Hg		Pb		C ₆ H ₁₀ O ₅		C ₄ H ₆ O ₄		C ₃₃ H ₃₂ O ₁₉												
	200.59	N/a	5.44	207.2	N/a	11.3	162	N/a	1.60	118	N/a	1.57	732	N/a	1.50						
	1	0	1.0000	1	0	1	5	0	1	4	0	1	19	0	1						
Double salts	Tri ammonium hydrogen disulfate		Tri sodium hydrogen disulfate		Tri potassium hydrogen disulfate																
	(NH ₄) ₃ H(SO ₄) ₂		Na ₃ H(SO ₄) ₂		K ₃ H(SO ₄) ₂																
	247	53.3	1.77	262	45.56	2.56	310	N/a	2.49												
	5	0.1466	1.7151	5	0.4556	1.2058	5	N/a	N/a												

Title Page	Abstract	Introduction
Conclusions	References	
Tables	Figures	
◀	▶	
◀	▶	
Back	Close	
Full Screen / Esc		
Printer-friendly Version		
Interactive Discussion		



**EQSAM4 model
description**

S. Metzger et al.

Table 2. RHD values at T_o and the T -coefficients for major salt compounds used to determine v_i .

Solute	NaCl	NaNO ₃	Na ₂ SO ₄	NH ₄ NO ₃	(NH ₄) ₂ SO ₄	NH ₄ HSO ₄
RHD(T_o)	0.7528	0.7379	0.930	0.6183	0.7997	0.400
T -coefficient	25.00	304.00	80.00	852.00	80.00	384.00
Solute	(NH ₄) ₃ H(SO ₄) ₂	NH ₄ Cl	NaHSO ₄	Ca(NO ₃) ₂	CaCl ₂	K ₂ SO ₄
RHD(T_o)	0.6900	0.7710	0.520	0.4906	0.2830	0.9750
T -coefficient	186.00	239.00	-45.00	509.40	551.10	35.60
Solute	KHSO ₄	KNO ₃	KCl	MgSO ₄	Mg(NO ₃) ₂	MgCl ₂
RHD(T_o)	0.860	0.9248	0.8426	0.8613	0.5400	0.3284
T -coefficient	00.00	00.00	159.00	-714.45	230.20	42.23

[Title Page](#)[Abstract](#)[Introduction](#)[Conclusions](#)[References](#)[Tables](#)[Figures](#)[◀](#)[▶](#)[◀](#)[▶](#)[Back](#)[Close](#)[Full Screen / Esc](#)[Printer-friendly Version](#)[Interactive Discussion](#)

EQSAM4 model description

S. Metzger et al.

Table 3. Relative humidity of deliquescence (RHD) at $T^o = 298$ [K]. Bold values represent measurements, non-bold values are obtained from Eqs. (3) and (1). All non-bold values are indicative (measurements are required for validation).

	PO_4^{3-}	SO_4^{2-}	HSO_4^-	NO_3^-	Cl^-	Br^-	I^-	CO_3^{2-}	HCO_3^-	OH^-	CHO_2^-	$\text{C}_2\text{H}_5\text{O}_2^-$	$\text{C}_2\text{O}_4^{2-}$	$\text{C}_6\text{H}_5\text{O}_7^{2-}$
H^+	N/a	N/a	--	N/a	N/a	N/a	N/a	N/a	--	N/a	N/a	N/a	N/a	N/a
NH_4^+	0.9321	0.7997	0.4001	0.6186	0.7711	0.7727	0.7468	0.7390	0.8493	1.0000	0.5837	0.6307	0.9485	0.6083
Na^+	0.9664	0.93	0.52	0.738	0.7528	0.7603	0.7488	0.8780	0.9064	0.5102	0.6642	0.7851	0.9542	0.9288
K^+	0.8661	0.975	0.86	0.9248	0.8427	0.8243	0.7959	0.7976	0.8586	0.5779	0.5103	0.5896	0.9182	0.4950
Ca^{2+}	0.7548	0.9554	--	0.4907	0.2831	0.8200	0.8406	0.9284	--	0.8869	0.9458	0.5941	0.9510	0.4951
Mg^{2+}	0.4223	0.861	--	0.5401	0.3284	0.8511	0.8705	0.9069	--	0.8393	0.4244	0.8553	0.4923	0.4956
Fe^{3+}	0.6973	0.8001	--	0.8997	0.8438	0.7429	0.9868	0.8249	--	0.7745	0.8742	0.4939	0.4952	0.4176
NH_3	$(\text{CH}_3)_2\text{CO}$	CH_3OH	$\text{CH}_3\text{CH}_2\text{OH}$	$\text{C}_6\text{H}_{12}\text{O}_6$	$\text{C}_6\text{H}_{14}\text{O}_6$	$\text{C}_{12}\text{H}_{22}\text{O}_{11}$	Hg	Pb	$\text{C}_6\text{H}_{10}\text{O}_5$	$\text{C}_4\text{H}_6\text{O}_4$	$\text{C}_{33}\text{H}_{32}\text{O}_{19}$	--	--	--
N/a	N/a	N/a	N/a	N/a	N/a	N/a	N/a	N/a	N/a	N/a	N/a	--	--	--
$(\text{NH}_4)_3\text{H}(\text{SO}_4)_2$	$\text{Na}_3\text{H}(\text{SO}_4)_2$	$\text{K}_3\text{H}(\text{SO}_4)_2$												
0.6901	0.9062	N/a												

[Title Page](#)[Abstract](#)[Introduction](#)[Conclusions](#)[References](#)[Tables](#)[Figures](#)[◀](#)[▶](#)[◀](#)[▶](#)[Back](#)[Close](#)[Full Screen / Esc](#)[Printer-friendly Version](#)[Interactive Discussion](#)

EQSAM4 model description

S. Metzger et al.

Table 4. Relative humidity of efflorescence (RHE) at $T = 298$ [K] and obtained with Eq. (2). All values are indicative (measurements are required for validation).

	PO_4^{3-}	SO_4^{2-}	HSO_4^-	NO_3^-	Cl^-	Br	I^-	CO_3^{2-}	HCO_3^-	OH^-	CHO_2^-	$\text{C}_2\text{H}_5\text{O}_2^-$	$\text{C}_2\text{O}_4^{2-}$	$\text{C}_6\text{H}_5\text{O}_3^-$
H^+	N/a	N/a	--	N/a	N/a	N/a	N/a	N/a	--	N/a	N/a	N/a	N/a	N/a
NH_4^+	0.8148	0.3291	0.0871	0.1223	0.7425	0.3423	0.0957	0.2610	0.9227	0.0177	0.2466	0.2012	0.9766	0.0261
Na^+	0.9621	0.6687	0.1469	0.3037	0.8410	0.2633	0.0900	0.7973	0.9882	0.4988	0.3631	0.6107	0.9733	0.2279
K^+	0.1203	0.0000	0.4911	0.2925	0.7077	0.3489	0.1031	0.1683	0.7511	0.3231	0.0835	0.0889	0.5691	0.0205
Ca^{2+}	0.0287	0.9725	--	0.2464	0.8569	0.0830	0.0457	0.9840	--	0.9906	0.9604	0.0398	0.9753	0.0185
Mg^{2+}	0.0206	0.7764	--	0.7636	0.9628	0.1436	0.0668	0.9882	--	0.9939	0.0378	0.3145	0.0472	0.0188
Fe^{3+}	0.0648	0.0258	--	0.1448	0.1850	0.0292	0.8906	0.3789	--	0.2720	0.1808	0.0263	0.0194	0.0211
NH_3	$(\text{CH}_3)_2\text{CO}$	CH_3OH	$\text{CH}_3\text{CH}_2\text{OH}$	$\text{C}_6\text{H}_{12}\text{O}_6$	$\text{C}_6\text{H}_{14}\text{O}_6$	$\text{C}_{12}\text{H}_{22}\text{O}_{11}$	Hg	Pb	$\text{C}_6\text{H}_{10}\text{O}_5$	$\text{C}_4\text{H}_6\text{O}_4$	$\text{C}_{33}\text{H}_{32}\text{O}_{19}$	--	--	
N/a	N/a	N/a	N/a	N/a	N/a	N/a	N/a	N/a	N/a	N/a	N/a	--	--	
$(\text{NH}_4)_3\text{H}(\text{SO}_4)_2$	$\text{Na}_3\text{H}(\text{SO}_4)_2$	$\text{K}_3\text{H}(\text{SO}_4)_2$												
0.2248	0.1318	N/a												

- [Title Page](#)
- [Abstract](#) | [Introduction](#)
- [Conclusions](#) | [References](#)
- [Tables](#) | [Figures](#)
- [◀](#) | [▶](#)
- [◀](#) | [▶](#)
- [Back](#) | [Close](#)
- [Full Screen / Esc](#)
- [Printer-friendly Version](#)
- [Interactive Discussion](#)



EQSAM4 model description

S. Metzger et al.

Table 5. Mixed solution domains (D1–10) to identify certain regimes, applied to determine x in Eq. (14).

Domain	t_X	/	t_Y	molar ratios of total X	to	total Y
D1	$t_{\text{cation(all)}}^+$	/	$t_{\text{anion(all)}}^-$	cations	to	anions
D2	$t_{\text{cation(all)}}^+$	/	$t_{\text{SO}_4}^{2-}$	cations	to	sulfate
D3	$t_{\text{cation(mineral)}}^+$	/	$t_{\text{SO}_4}^{2-}$	mineral cations	to	sulfate
D4	t_{Ca}^{2+}	/	$t_{\text{SO}_4}^{2-}$	calcium	to	sulfate
D5	t_{Mg}^{2+}	/	$t_{\text{SO}_4}^{2-}$	magnesium	to	sulfate
D6	t_{K}^+	/	$t_{\text{SO}_4}^{2-}$	potassium	to	sulfate
D7	t_{Na}^+	/	$t_{\text{SO}_4}^{2-}$	sodium	to	sulfate
D8	$t_{\text{NH}_4}^+$	/	$t_{\text{SO}_4}^{2-}$	ammonium	to	sulfate
D9	t_{Cl}^-	/	$t_{\text{SO}_4}^{2-}$	chloride	to	sulfate
D10	$t_{\text{NO}_3}^-$	/	$t_{\text{SO}_4}^{2-}$	nitrate	to	sulfate

[Title Page](#)

[Abstract](#)

[Introduction](#)

[Conclusions](#)

[References](#)

[Tables](#)

[Figures](#)

◀

▶

◀

▶

[Back](#)

[Close](#)

[Full Screen / Esc](#)

[Printer-friendly Version](#)

[Interactive Discussion](#)

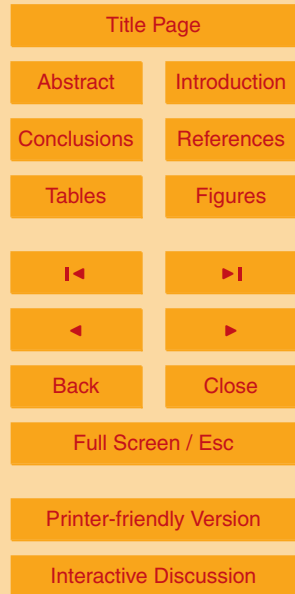


**EQSAM4 model
description**

S. Metzger et al.

Table 6. Mixed solution regimes (R1–6) that apply to each of the 10 domains listed in Table 5. X and Y either refer to the total of cations or anions, depending on the domain listed in Table 5.

Regime	X	to	Y	threshold	classification
R1	t_X	/	t_Y	> 2	X very rich
R2	t_X	/	t_Y	> 1	X rich
R3	t_X	/	t_Y	$\leq 1 $	X neutral
R4	t_X	/	t_Y	< -1	X poor
R5	t_X	/	t_Y	< -2	X very poor
R6	t_X	/	t_Y	≤ -3	no X



EQSAM4 model description

S. Metzger et al.

[Title Page](#)[Abstract](#)[Introduction](#)[Conclusions](#)[References](#)[Tables](#)[Figures](#)[◀](#)[▶](#)[◀](#)[▶](#)[Back](#)[Close](#)[Full Screen / Esc](#)[Printer-friendly Version](#)[Interactive Discussion](#)

Table 7. Solution cases that identify combinations of concentration regimes according to Tables 5 and 6. The cases specify the activity coefficient exponent x for the two volatile salt compounds, i.e. NH_4NO_3 and NH_4Cl in mixed solutions (for the other salt compounds of Table 1 no cases are applied). Note that the following definitions refer to Table 6: sulfate very rich equals R5; sulfate rich, R4; sulfate neutral, R3; sulfate poor, R2; sulfate very poor, R1. Pure compound refers to a single solute solution.

Domain	D8	D10	D7	D6	D4	D5	$x_{\text{NH}_4\text{NO}_3}$	$x_{\text{NH}_4\text{Cl}}$
Case	NH_4^+	NO_3^-	Na^+	K^+	Ca^{2+}	Mg^{2+}	RHD RH	RHD RH
C0	sulfate very rich				2.00 2.00		6.00 6.00	
C1–5	sulfate rich				2.00 2.00		6.00 6.00	
C6–10	sulfate neutral				2.00 2.00		6.00 6.00	
C10	R4	R2	R5	R5	R5	R5	0.00 0.50	0.00 0.50
C10–20	sulfate poor				2.00 2.00		6.00 6.00	
C11	R2	R4	R6	R6	R6	R6	0.00 0.50	0.00 0.50
C12	R2	R2	R6	R6	R6	R6	0.50 0.50	0.00 0.50
C13	R4	R4	R5	R6	R6	R6	0.00 1.00	0.00 8.00
C14	R2	R4	R5	R6	R6	R6	0.00 0.25	0.00 0.50
C15	R2	R4	R2	R6	R6	R6	1.000 0.125	2.00 0.25
C16	R4	R4	R5	R5	R5	R5	0.00 1.00	0.00 6.00
C17	R2	R4	R5	R5	R5	R5	2.00 0.25	0.00 0.50
C18	R2	R4	R2	R5	R5	R5	1.000 0.125	2.00 0.25
C19	R2	R4	R6	R5	R5	R5	2.00 0.25	2.00 0.25
C20	R2	R2	R6	R5	R5	R5	0.75 0.25	0.75 0.25
C1–9	sulfate very poor				2.00 2.00		6.00 6.00	
C21	R3	R6	R4	R6	R6	R6	0.25 0.25	0.25 0.25
C22	R2	R4	R4	R6	R6	R6	0.25 0.25	0.25 0.25
C23	pure compound				0.25 0.25		0.25 0.25	

EQSAM4 model description

S. Metzger et al.

[Title Page](#)[Abstract](#)[Introduction](#)[Conclusions](#)[References](#)[Tables](#)[Figures](#)[◀](#)[▶](#)[◀](#)[▶](#)[Back](#)[Close](#)[Full Screen / Esc](#)[Printer-friendly Version](#)[Interactive Discussion](#)

EQSAM4 model description

S. Metzger et al.

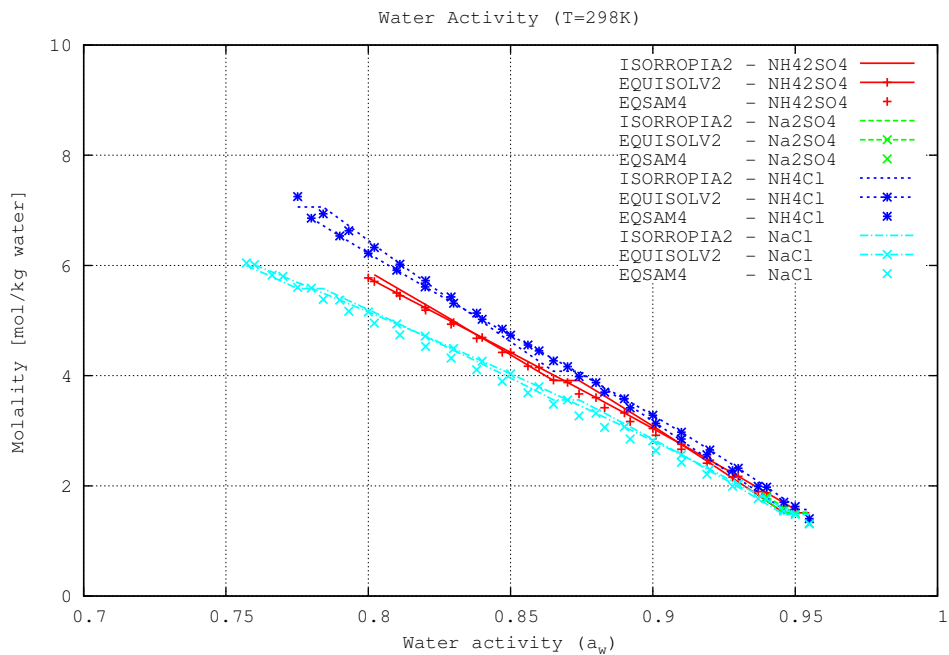


Fig. 1a. Single solute molality as a function of water activity for several electrolytes: $(\text{NH}_4)_2\text{SO}_4$, Na_2SO_4 , NH_4Cl , NaCl (at $T=298.15\text{ K}$) calculated with EQSAM4 from Eq. (1) and compared to tabulated data used in ISORROPIA II and EQUISOLV II.

- [Title Page](#)
- [Abstract](#) [Introduction](#)
- [Conclusions](#) [References](#)
- [Tables](#) [Figures](#)
- [◀](#) [▶](#)
- [◀](#) [▶](#)
- [Back](#) [Close](#)
- [Full Screen / Esc](#)
- [Printer-friendly Version](#)
- [Interactive Discussion](#)



EQSAM4 model description

S. Metzger et al.

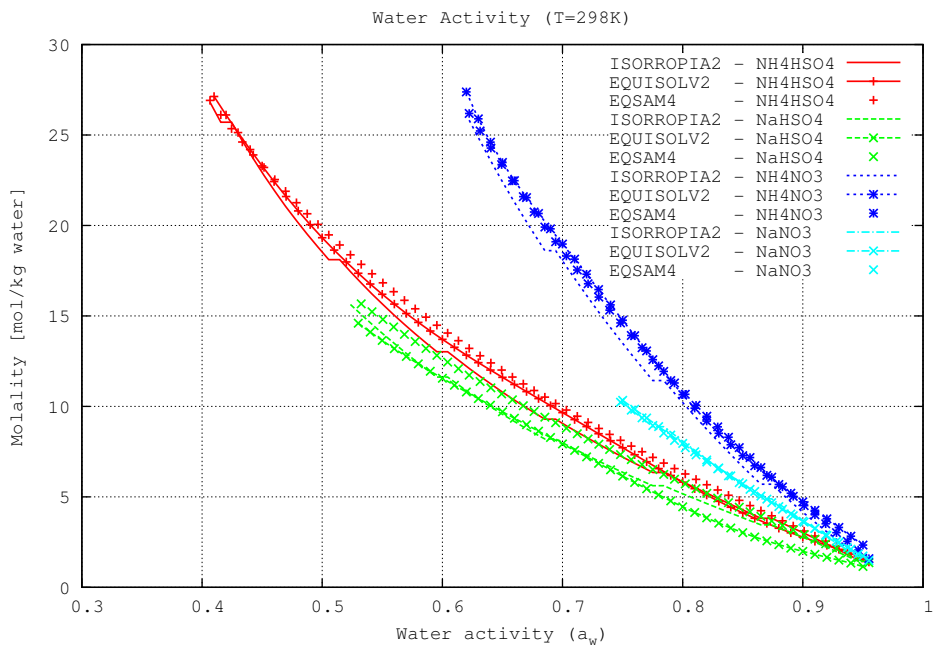
[Title Page](#)[Abstract](#)[Introduction](#)[Conclusions](#)[References](#)[Tables](#)[Figures](#)[◀](#)[▶](#)[◀](#)[▶](#)[Back](#)[Close](#)[Full Screen / Esc](#)[Printer-friendly Version](#)[Interactive Discussion](#)

Fig. 1b. Same as Fig. 1a for $(\text{NH}_4)\text{HSO}_4$, NaHSO_4 , NH_4NO_3 , NaNO_3 (at $T = 298.15 \text{ K}$).

EQSAM4 model description

S. Metzger et al.

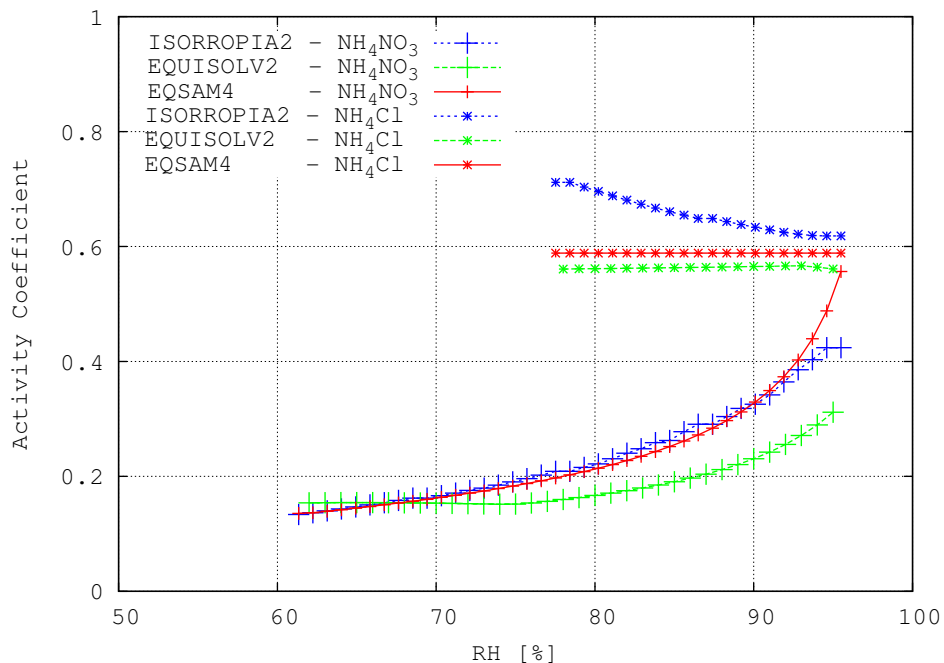


Fig. 2. Binary activity coefficient of NH_4NO_3 and NH_4Cl at $T = 298$ [K]; obtained for EQSAM4 as a function of solute molality and RH with Eq. (8). The values used by ISORROPIA II (Fountoukis and Nenes, 2007) and EQUISOLV II (Jacobson, 1999) are included for comparison.

- [Title Page](#)
- [Abstract](#) [Introduction](#)
- [Conclusions](#) [References](#)
- [Tables](#) [Figures](#)
- [◀](#) [▶](#)
- [◀](#) [▶](#)
- [Back](#) [Close](#)
- [Full Screen / Esc](#)
- [Printer-friendly Version](#)
- [Interactive Discussion](#)



EQSAM4 model description

S. Metzger et al.

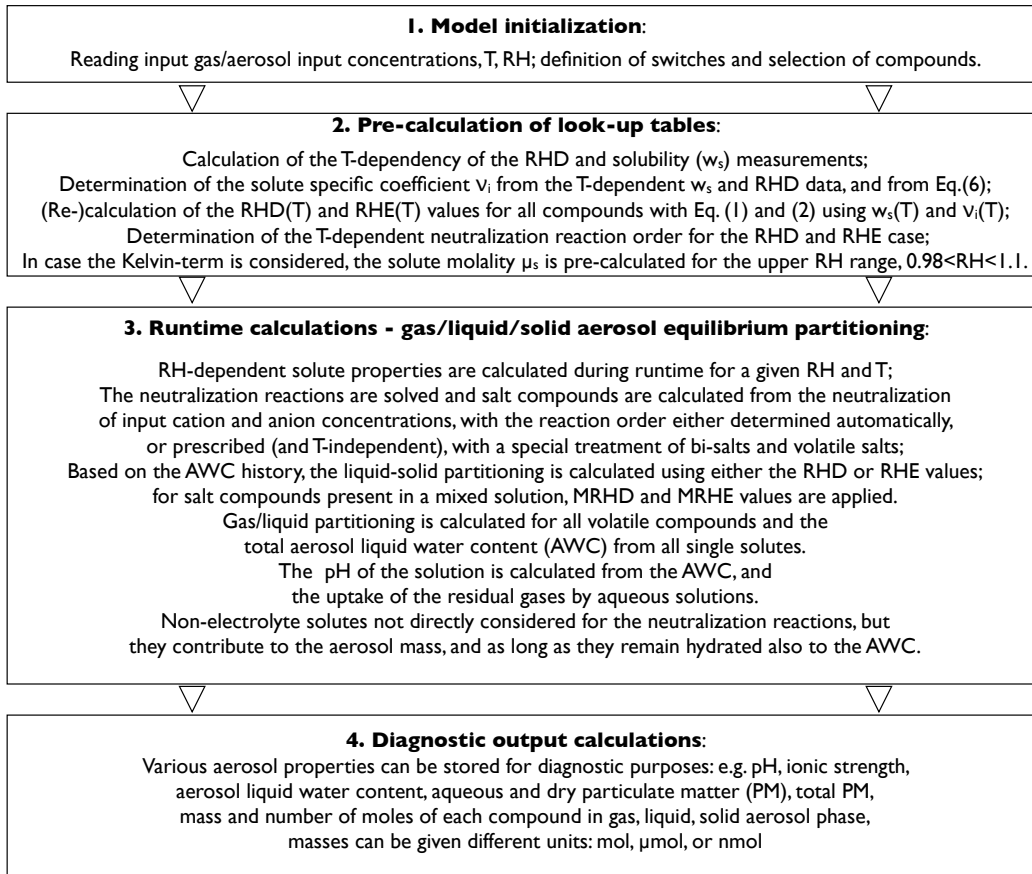


Fig. 3. Generic solution procedure of EQSAM4.

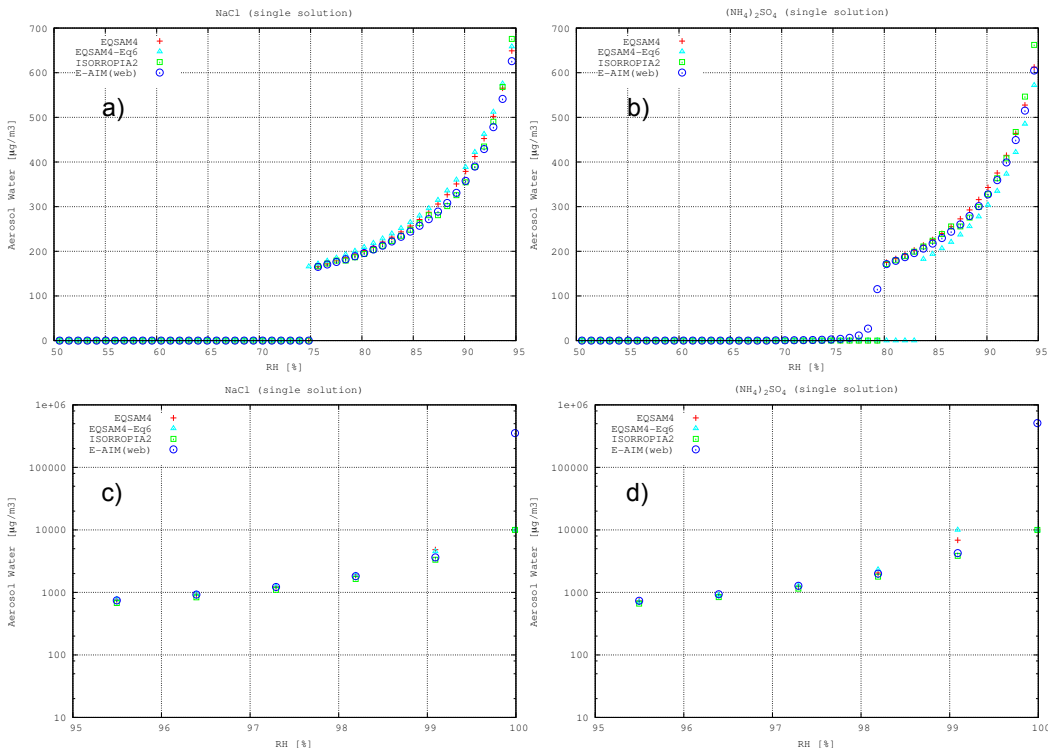


Fig. 4a–d. Water uptake of atmospheric aerosols – single salt solutions fixed to 1 $\mu\text{mol}(\text{solute})/\text{m}^3(\text{air})$: (a, c) $\text{NaCl}-\text{H}_2\text{O}$ and (b, d) $(\text{NH}_4)_2\text{SO}_4-\text{H}_2\text{O}$, with (a, b) $\text{RH} \leq 95\%$ [%] and (c, d) $\text{RH} \geq 95\%$ [%], showing EQSAM4 (red crosses) versus E-AIM (web version) (blue circles) and ISORROPIA II (green squares).

EQSAM4 model description

S. Metzger et al.

[Title Page](#)

[Abstract](#)

[Introduction](#)

[Conclusions](#)

[References](#)

[Tables](#)

[Figures](#)

◀

▶

◀

▶

[Back](#)

[Close](#)

[Full Screen / Esc](#)

[Printer-friendly Version](#)

[Interactive Discussion](#)



EQSAM4 model description

S. Metzger et al.

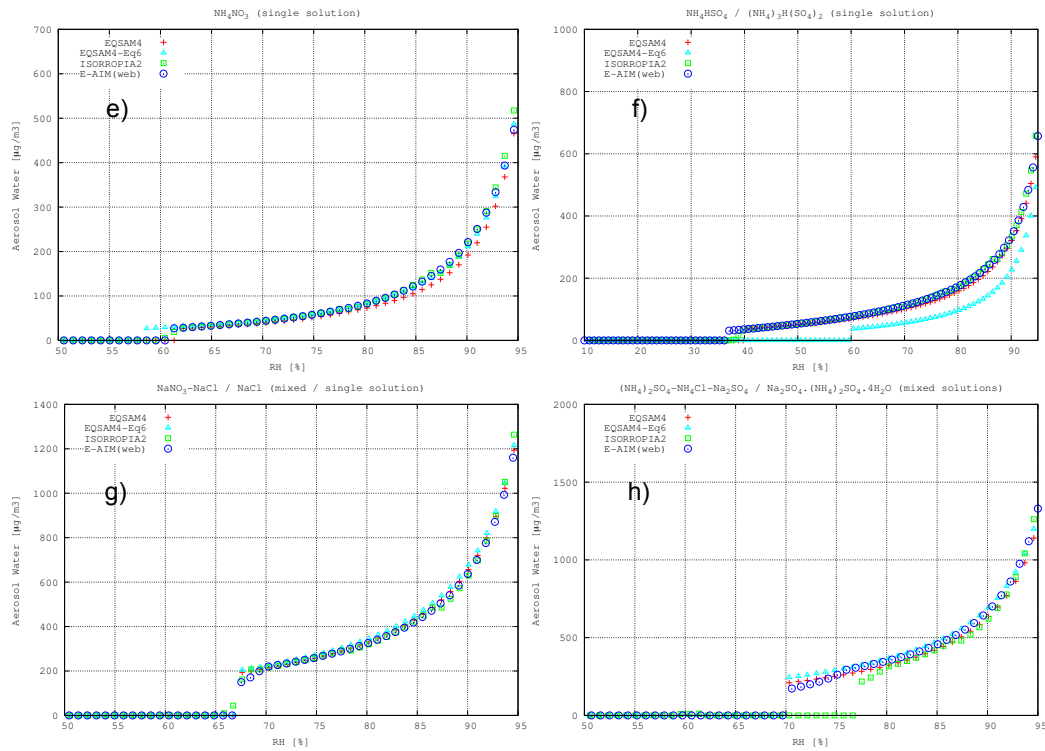


Fig. 4e–h. Continued. Single salt solutions of (e) $\text{NH}_4\text{NO}_3\text{-H}_2\text{O}$ and (f) $\text{NH}_4\text{HSO}_4\text{-H}_2\text{O}$, and corresponding mixed solutions of (g) $\text{NaNO}_3\text{-NaCl-H}_2\text{O}$ and (h) $(\text{NH}_4)_2\text{SO}_4\text{-NH}_4\text{Cl-Na}_2\text{SO}_4\text{-H}_2\text{O}$. All single solute concentrations were fixed to 1 [$\mu\text{mol}/\text{m}^3(\text{air})$], and the same MRHD values as used in ISORROPIA II have been applied for the mixed solution cases.

[Title Page](#)

[Abstract](#)

[Introduction](#)

[Conclusions](#)

[References](#)

[Tables](#)

[Figures](#)

[◀](#)

[▶](#)

[◀](#)

[▶](#)

[Back](#)

[Close](#)

[Full Screen / Esc](#)

[Printer-friendly Version](#)

[Interactive Discussion](#)



[Title Page](#)

[Abstract](#)

[Introduction](#)

[Conclusions](#)

[References](#)

[Tables](#)

[Figures](#)

◀

▶

◀

▶

[Back](#)

[Close](#)

[Full Screen / Esc](#)

[Printer-friendly Version](#)

[Interactive Discussion](#)

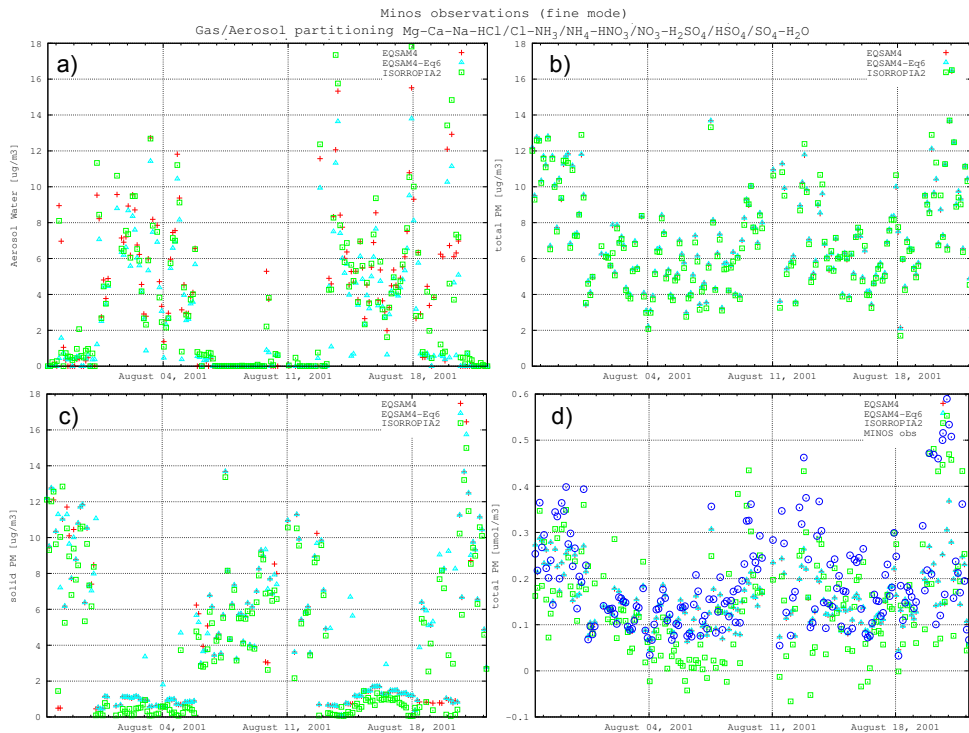


Fig. 5a–d. MINOS Campaign. Aerosol fine mode. Mixed solution properties and model comparison, following Metzger et al. (2006). **(a)** Aerosol water mass [$\mu\text{g}/\text{m}^3(\text{air})$], **(b)** total particulate matter (PM) [$\mu\text{g}/\text{m}^3(\text{air})$], **(c)** total solid matter (PM) [$\mu\text{g}/\text{m}^3(\text{air})$], **(d)** total number of moles of (PM) [$\mu\text{mol}/\text{m}^3(\text{air})$]. All panels show time series for the period 28 July–25 August 2001 and show the EQSAM4 results based on v_i determined from the compound RHD (red crosses), EQSAM4-Eq6 based on v_i estimated from Eq. (6) (turquoise triangles), ISORROPIA II (green open squares). Measurements are included, if available (blue open circles).

EQSAM4 model description

S. Metzger et al.

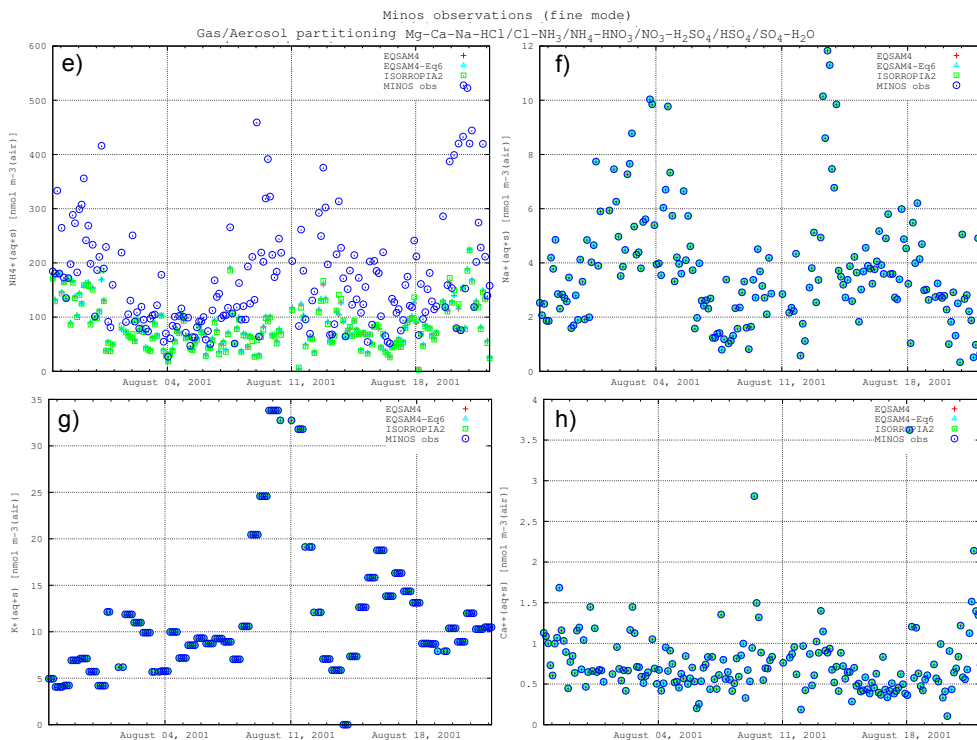


Fig. 5e–h. Continued. (e) total particulate ammonium, (f) total particulate sodium, (g) total particulate potassium, (h) total particulate calcium. All concentration are in $[\text{nmol}/\text{m}^3(\text{air})]$.

[Title Page](#)[Abstract](#)[Introduction](#)[Conclusions](#)[References](#)[Tables](#)[Figures](#)[◀](#)[▶](#)[◀](#)[▶](#)[Back](#)[Close](#)[Full Screen / Esc](#)[Printer-friendly Version](#)[Interactive Discussion](#)

EQSAM4 model description

S. Metzger et al.

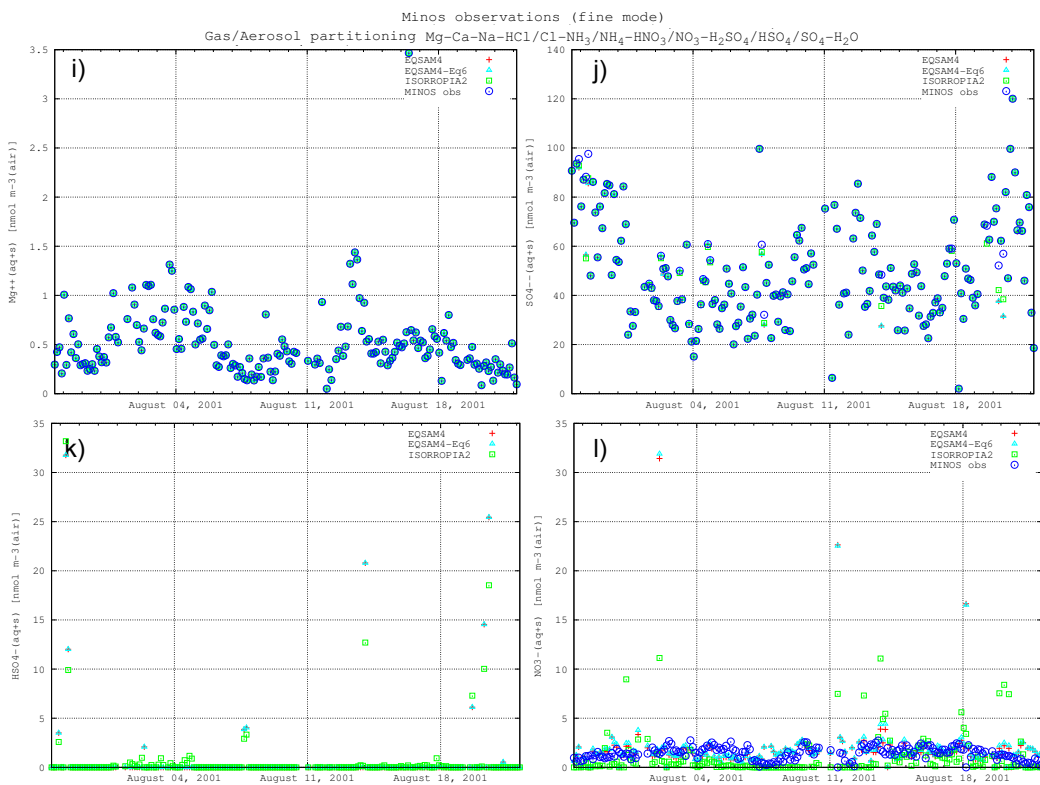


Fig. 5i–l. Continued. (i) total particulate magnesium, (j) total particulate sulfate, (k) total particulate bi-sulfate, (l) total particulate nitrate. All concentration are in [nmol/m³(air)].

[Title Page](#)[Abstract](#)[Introduction](#)[Conclusions](#)[References](#)[Tables](#)[Figures](#)[◀](#)[▶](#)[◀](#)[▶](#)[Back](#)[Close](#)[Full Screen / Esc](#)[Printer-friendly Version](#)[Interactive Discussion](#)

EQSAM4 model description

S. Metzger et al.

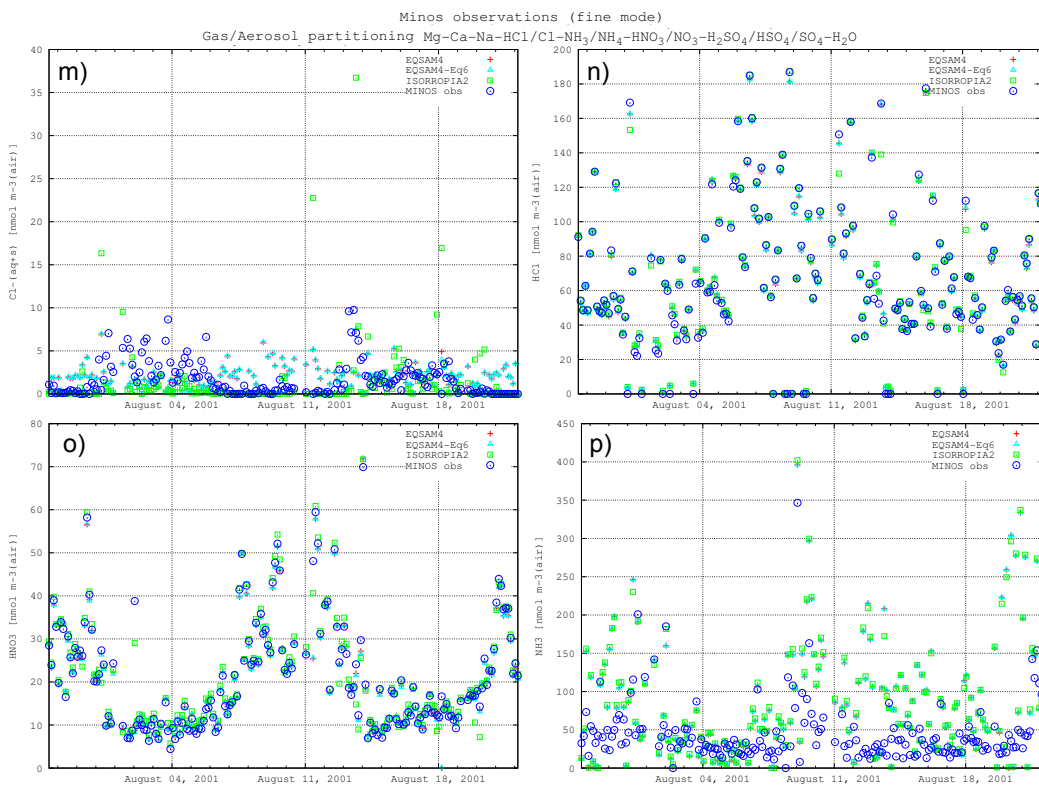


Fig. 5m–p. Continued. **(m)** total particulate chloride, **(n)** residual gaseous HCl, **(o)** residual gaseous HNO₃, **(p)** residual gaseous NH₃. All concentration are in [nmol/m³(air)].

[Title Page](#)[Abstract](#)[Introduction](#)[Conclusions](#)[References](#)[Tables](#)[Figures](#)[◀](#)[▶](#)[◀](#)[▶](#)[Back](#)[Close](#)[Full Screen / Esc](#)[Printer-friendly Version](#)[Interactive Discussion](#)

EQSAM4 model description

S. Metzger et al.

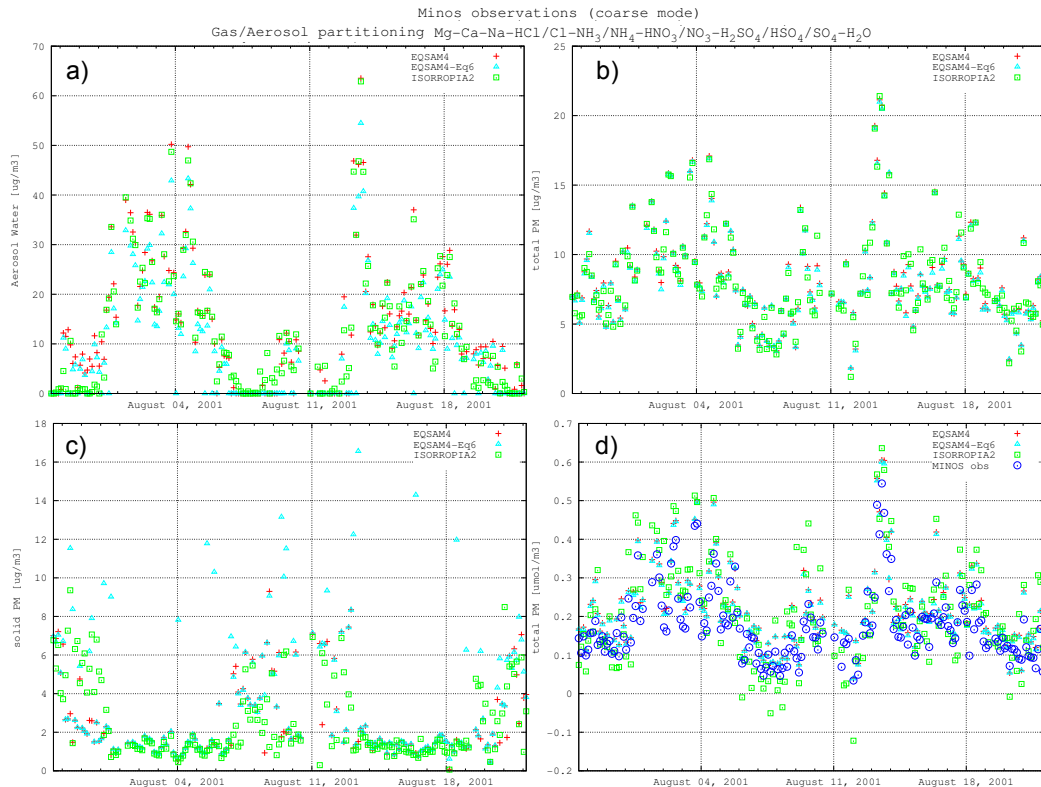


Fig. 6a–d. As Fig. 5 with results for the aerosol coarse mode. **(a)** Aerosol water mass [$\mu\text{g}/\text{m}^3(\text{air})$], **(b)** total particulate matter (PM) [$\mu\text{g}/\text{m}^3(\text{air})$], **(c)** total solid matter (PM) [$\mu\text{g}/\text{m}^3(\text{air})$], **(d)** total number of moles of (PM) [$\mu\text{mol}/\text{m}^3(\text{air})$].

[Title Page](#)

[Abstract](#)

[Introduction](#)

[Conclusions](#)

[References](#)

[Tables](#)

[Figures](#)

◀

▶

◀

▶

[Back](#)

[Close](#)

[Full Screen / Esc](#)

[Printer-friendly Version](#)

[Interactive Discussion](#)

EQSAM4 model description

S. Metzger et al.

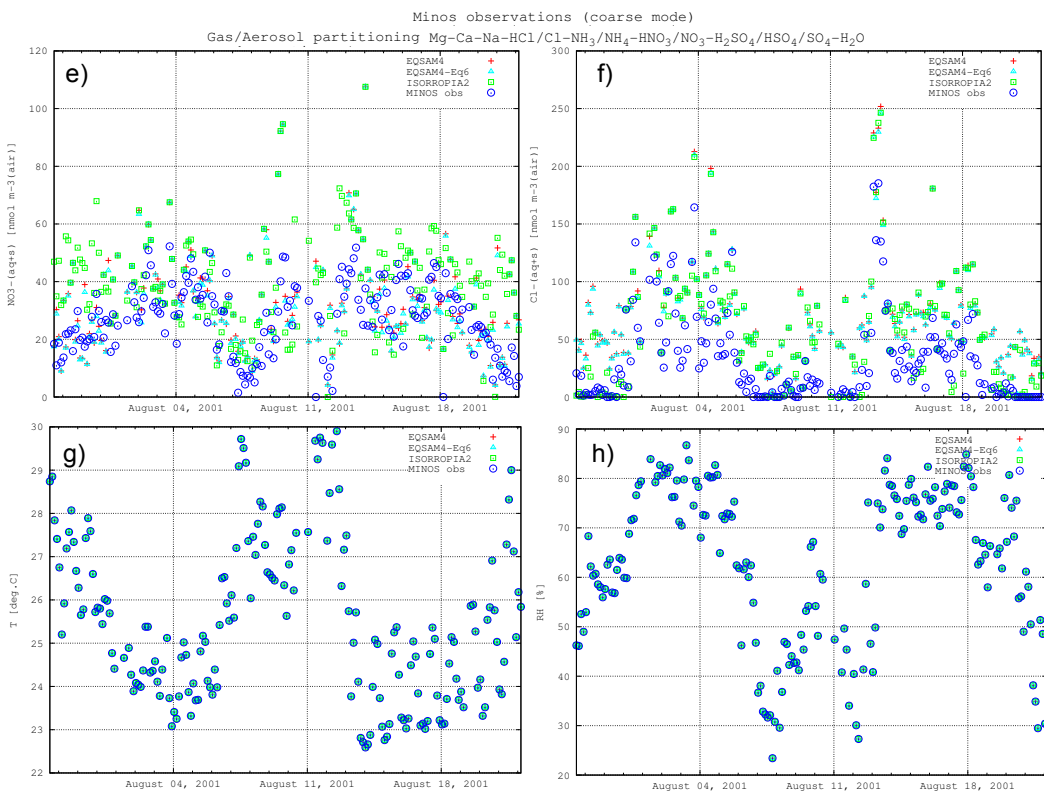


Fig. 6e–h. Continued. (e) total particulate nitrate [$\text{nmol}/\text{m}^3(\text{air})$], (f) particulate chloride [$\text{nmol}/\text{m}^3(\text{air})$], (g) observed temperature [$^\circ\text{C}$], (h) observed relative humidity [%].

[Title Page](#)[Abstract](#)[Introduction](#)[Conclusions](#)[References](#)[Tables](#)[Figures](#)[◀](#)[▶](#)[◀](#)[▶](#)[Back](#)[Close](#)[Full Screen / Esc](#)[Printer-friendly Version](#)[Interactive Discussion](#)

EQSAM4 model description

S. Metzger et al.

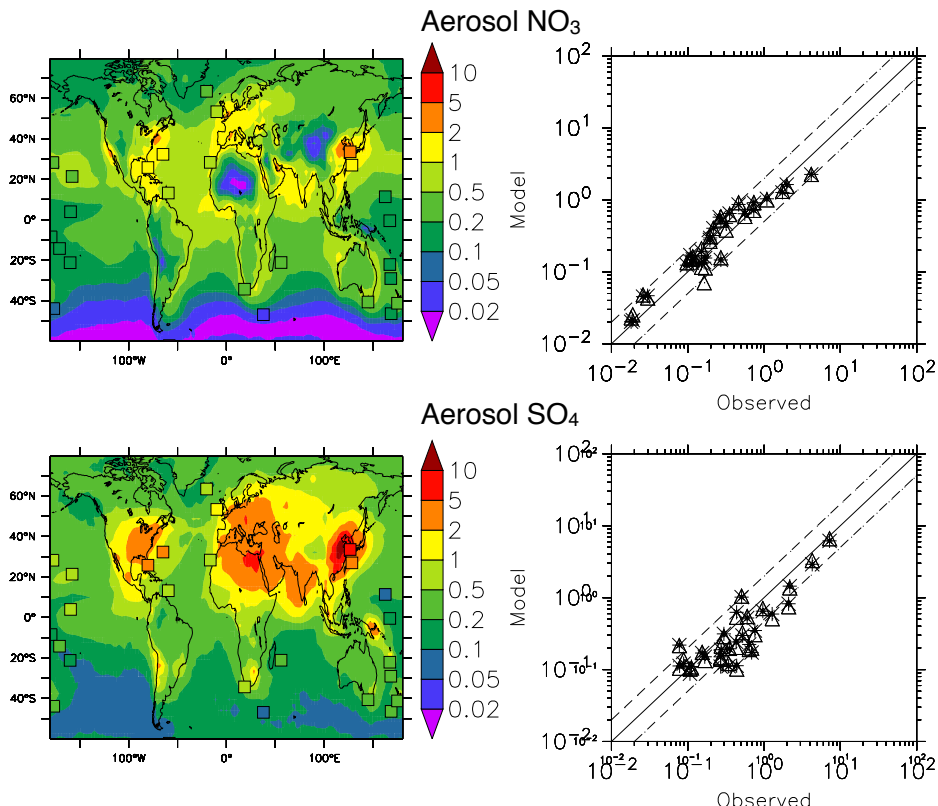


Fig. 7. Comparison of model results to data collected in AEROCE. Maps show surface concentrations of nitrate (top) and sulfate (bottom) for the year 2002 simulated using EQSAM4. The over-plotted squares represent data from AEROCE. Scatter plots show the comparison of model vs. AEROCE data for nitrate (top) and sulfate (bottom); observations are included for the year 2001 (triangles) and 2002 (stars). Units are [$\mu\text{g}/\text{m}^3(\text{air})$].

**EQSAM4 model
description**

S. Metzger et al.

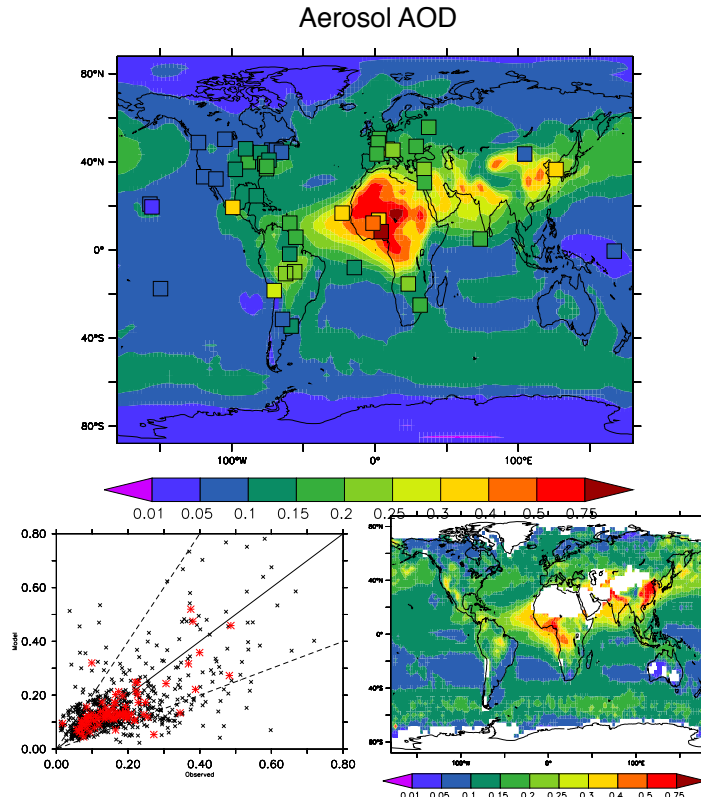


Fig. 8. (Top) Annual mean AOD modeled with GMXe for the year 2001; over-plotted are annual mean measurements from the AERONET network (2001). (Bottom left) Summary of the comparison between GMXe using EQSAM4 and AERONET, black crosses are monthly means and red annual means ($r^2 = 0.51$). (Bottom right) Annual mean AOD from MODIS for the year 2001. Figures 7 and 8 complement Figs. 14 and 15 of Pringle et al. (2010).

[Title Page](#)[Abstract](#)[Introduction](#)[Conclusions](#)[References](#)[Tables](#)[Figures](#)[◀](#)[▶](#)[◀](#)[▶](#)[Back](#)[Close](#)[Full Screen / Esc](#)[Printer-friendly Version](#)[Interactive Discussion](#)